Pulse Shaping Design for PAPR Reduction in OFDM

by

Akansha Jain

200711010

A thesis submitted in the partial fulfillment of the requirements for the degree of
Master of Technology
in
Information and Communication Technology

Dhirubhai Ambani Institute of
Information and Communication Technology, Gandhinagar

May 2009

Declaration

This is to certify that

1. The thesis comprises my original work towards the degree of **Master of Technology** in **Information and Communication Technology at DA-IICT** and has not been submitted elsewhere for a degree.
2. Due acknowledgement has been made in the text to all other material used.

Signature of student

Akansha Jain

Certificate

This is to certify that the thesis work entitled **"Pulse Shaping Design for PAPR Reduction in OFDM "** has been carried out by **Akansha Jain (200711010)** for the degree of Master of Technology in Information and Communication Technology at this Institute under my supervision.

Prof. C. Vijaykumar

Dedicated to the fond memory of my Grandmother

Acknowledgements

First and foremost I take the opportunity to express my profound gratitude to my adviser and idea-generator Prof. C. Vijaykumar, for his continuing support and guidance. His limitless patience and the sharpening and thought provoking discussions with him have been invaluable throughout my studies.

I would like to express my sincere thanks to my thesis examiners Prof. S. C. Sahasrabudhe and Prof. V. P. Sinha for their valuable advice which helped me to fortify my foundations. I am highly indebted to Prof. V. P. Sinha for the encouraging discussions on the abstract notions of linear algebra and signal processing.

It is my distinct pleasure to thank my friends especially, Pankesh Patel,Divyang Rawal, Nilesh Banker,I Naga Vishnukant ,who directly or indirectly helped me to successfully complete my MTech.thesis.

Finally, I would give my deepest appreciation to my family members for their constant love and for providing me with the opportunity and the encouragement to pursue my goals.

Abstract

Future mobile communications systems reaching for ever increasing data rates require higher bandwidths than those typical used in todays cellular systems. By going to higher bandwidth the (for low bandwidth) flat fading radio channel becomes frequency selective and time dispersive. Due to its inherent robustness against time dispersion Orthogonal Frequency Division Multiplex (OFDM) is an attractive candidate for such future mobile communication systems. OFDM partitions the available bandwidth into many subchannels with much lower bandwidth. Such a narrowband subchannel experiences now almost flat fading channel. However, one potential drawback with OFDM modulation is the high Peak to Average Power Ratio (PAPR) of the transmitted signal: The signal transmitted by the OFDM system is the superposition of all signals transmitted in the narrowband subchannels. The transmit signal has then due to the central limit theorem a Gaussian distribution leading to high peak values compared to the average power. A system design not taking this into account will have a high clip rate. Each signal sample that is beyond the saturation limit of the power amplifier suffers either clipping to this limit value or other non- linear distortion, both creating additional bit errors in the receiver. One possibility to avoid clipping is to design the system for very high signal peaks. However, this approach leads to very high power consumption (since the power amplifier must have high supply rails) and also complex power amplifiers. The preferred solution is therefore to apply digital signal processing that reduces such high peak values in the transmitted signal thus avoiding clipping. These methods are commonly referred to as PAPR reduction. PAPR reduction methods can be categorized into transparent methods here the receiver is not aware of the reduction scheme applied by the transmitter and non-transparent methods where the receiver needs to know the PAPR algorithm applied by the transmitter. This master thesis would focus on transparent PAPR reduction algorithms. The pulse shaping mechanism is used to reduce PAPR . The effect is analyzed in terms of BER.

Contents

Acknowledgements iv

Abstract v

List of Figures ix

List of Tables xi

Abbreviations xii

1 Introduction 1
- 1.1 Motivation . . . 1
- 1.2 Outline of the thesis . . . 2
  - 1.2.1 Multirate Systems and Filter Banks (Chapter 2) . . . 2
  - 1.2.2 OFDM and Filter Bank Based Multicarrier ModulationSystems (Chapter 3) . . . 2
  - 1.2.3 PAPR Reduction Methods and Pulse Shaping (Chapter 4) . 3
  - 1.2.4 Discussion on Simulation Results (Chapter 5) . . . 3
- 1.3 Notations . . . 3

2 Multirate Systems and Filter Banks 5
- 2.1 Fundamental concepts . . . 6
  - 2.1.1 Basic building blocks . . . 6
    - 2.1.1.1 Interpolator . . . 6
    - 2.1.1.2 Decimator . . . 7
  - 2.1.2 Multirate identities and polyphase structure . . . 8
    - 2.1.2.1 The noble identities . . . 8
    - 2.1.2.2 Polyphase representation . . . 9
- 2.2 Multirate filter banks . . . 9
  - 2.2.1 Uniform DFT filter banks . . . 10
    - 2.2.1.1 Polyphase implementations of two-channel structures 12
    - 2.2.1.2 Polyphase implementation of M-channel structures 13
- 2.3 Multirate systems and digital communications . . . 15
  - 2.3.1 Transmultiplexers (TMUX) . . . 16

2.3.2 TMUX in terms of polyphase matrices 18

3 OFDM and Filter Bank based Multicarrier Systems 20
3.1 Overview of OFDM system 21
3.1.1 OFDM Modulator 22
3.1.2 Demodulator 23
3.1.2.1 Disadvantages: 23
3.1.3 DFT Based Digital OFDM 24
3.1.4 IFFT Based Modulator 26
3.1.5 Demodulator 27
3.2 OFDM using multirate systems 28
3.3 Advantages of OFDM System 29
3.4 Disadvantages of OFDM system 30
3.5 What is the solution 31

4 PAPR Reduction Methods and Pulse Shaping 34
4.1 Peak To Average Power Ratio 35
4.2 Mathematical definition of PAPR 36
4.3 PAPR Reduction Methods 37
4.3.1 Transparent methods 37
4.3.1.1 Clipping 38
4.3.1.2 Tone Reservation 38
4.3.1.3 Active Constellation extension 39
4.3.2 Non Transparent Methods 39
4.3.2.1 Coding Schemes 40
4.3.2.2 Phase Optimization Techniques 40
4.3.2.3 Tone Injection 41
4.3.3 Wireless channel model and its power delay profile[32] 42
4.4 Pulse shaping and Nyquist filter design 43
4.4.1 Design of transmit and receive filter to meet Nyquist criterion 46
4.4.1.1 Problem formulation 47
4.4.1.2 Design procedure 50

5 Discussion on Simulation Results 54
5.1 Simulation Results 54
5.1.1 PAPR Using Clipping 55
5.1.2 PAPR for BPSK modulation 56
5.1.3 PAPR for 16-QAM modulation 58
5.1.4 PAPR for 64-QAM modulation 60
5.1.5 PAPR for 256-QAM modulation 62
5.1.6 RF Amplifier Characteristics 64

6 Conclusion and Direction 67
6.1 Conclusion 67

6.2 Future Direction 67

A Power Delay Profile of Channels **69**

Bibliography **70**

List of Figures

2.1 The basic multirate building blocks 6
2.2 Transform domain effect of interpolator 7
2.3 Demonstration of aliasing effect for M=2 8
2.4 Noble identities for multirate systems 8
2.5 (a) Analysis filter bank (b) Synthesis filter bank (c) Typical response of uniform DFT filter bank for M=4 10
2.6 A uniform DFT analysis filter bank 11
2.7 Two-channel QMF bank 13
2.8 (a)Redrawing the two-channel QMF bank (b)$P(z) = R(z)E(z)$ . . . 13
2.9 Trivial perfect reconstruction system 13
2.10 M-channel QMF bank 14
2.11 Redrawing of M-channel QMF bank with polyphase matrices 14
2.12 (a)$P(z) = R(z)E(z)$ (b) A structure equivalent to (a) when $E(z)$ is lossless 14
2.13 Digital communication system 16
2.14 Transmultiplexer structure drawn in terms of filer bank notations . 16
2.15 Equivalent structure for the TMUX in terms of polyphase matrices 18

3.1 Comparison of spectral efficiency of OFDM with that of conventional FDM 22
3.2 OFDM modulator 22
3.3 OFDM Demodulator 23
3.4 PSD of OFDM signal for four subcarriers without virtual carriers . 25
3.5 PSD of OFDM signal for 52 subcarriers without virtual subcarriers 25
3.6 PSD of OFDM signal for 52 subcarriers plus six virtual subcarriers on each side 26
3.7 IFFT based modulator 26
3.8 FFT based demodulator 27
3.9 Multiplexing operation of OFDM regarded as synthesis filter bank of TMUX 29
3.10 Notations: (a)Blocking and (b)Unblocking operations 29
3.11 OFDM transmitting system with increased symbol rate 31
3.12 Filter bank transceiver 32

4.1 Power delay profile of channel reampled by $\frac{M}{N}$ 43

4.2 Demonstration of effect of channel for N=3 and M=3. **(a)**original signal convolved with channel **(a)**Upsampled signal convolved with channel 44
4.3 Interpolation filter $w(n)$ and its equivalent polyphase representation 45
4.4 Nyquist(M) property of $G(Z)$ demonstrated for M=3 45
4.5 Considered digital equivalent of the communication channel. **(a)**Cascade of interpolator and decimator **(b)**Redrwaing in polyphse form **(c)**Basic multirate identity **(d)**Simplification of part (b) using the identity . 46

5.1 BER performance using clipping and Square Root Nyquist(M)filter 56
5.2 BER for BPSK modulation with oversampling factor M=4 57
5.3 BER for BPSK modulation with oversampling factor M=6 57
5.4 BER for BPSK modulation with oversampling factor M=8 58
5.5 BER for 16-QAM modulation with oversampling factor M=4 59
5.6 BER for 16-QAM modulation with oversampling factor M=6 59
5.7 BER for 16-QAM modulation with oversampling factor M=8 60
5.8 BER for 64-QAM modulation with oversampling factor M=4 61
5.9 BER for 64-QAM modulation with oversampling factor M=6 61
5.10 BER for 64-QAM modulation with oversampling factor M=8 62
5.11 BER for 256-QAM modulation with oversampling factor M=4 . . . 63
5.12 BER for 256-QAM modulation with oversampling factor M=6 . . . 63
5.13 BER for 256-QAM modulation with oversampling factor M=8 . . . 64
5.14 Gain characteristics of amplifier 65
5.15 PIN vs POUT characteristics of amplifier with Nyquist(M) filter . . 65
5.16 PIN vs POUT characteristics of amplifier with Raised Cosine filter . 66
5.17 PIN vs POUT characteristics of amplifier with out filter 66

List of Tables

5.1 Simulaion Parameters for IEEE802.11a PHY(Physical Layer) 55
5.2 PAPR for BPSK modulation 56
5.3 PAPR for 16-QAM modulation 58
5.4 PAPR for 64-QAM modulation 60
5.5 PAPR for 256-QAM modulation 62

A.1 Power-Delay Profile of ETSI[2] channel 69
A.2 Power-Delay Profile of JTC[B] channel 69

Abbreviations

ADSL	Assymetric Digital Subscriber Lines
WLAN	Wireless Local Area Network
PR	Perfect Reconstruction
MIMO	Multi Input Multi Output
OFDM	Orthogonal Frequency Division Multiplexing
FIR	Finite Impulse Response
QMF	Quadrature Mirror Filter
TMUX	Transmultiplexer
ISI	Inter Symbol Interference
PAPR	Peak to Average Power Ratio
CP	Cyclic Prefix
IDFT	Inverse Discrete Fourier Transform
ADC	Analog to Digital Converter
FFT	Fast Fourier Transform
LTI	Linear Time Invariant
RF	Radio Frequency
BER	Bit Error Rate
SNR	Signal to Noise Ratio

Chapter 1

Introduction

1.1 Motivation

The performance of high data rate systems are significantly limited by the multipath interference that occurs in the radio channel environment. Orthogonal Frequency Division Multiplexing(OFDM) is widely used to mitigate the effect of ISI in frequency selective channel[11, 12, 13]. OFDM is widely used in asymmetrical digital subscriber lines(ADSL),wireless local area network(WLAN) etc. Due the significant presence of multirate signal processing in the context of filter banks[1, 2, 3, 4] OFDM system has been implemented as transmultiplexers using multirate filter banks[7].These play a very important role in signal decomposition, analysis, modeling and, reconstruction[5, 6].

The thesis mainly concentrates on the reduction of Peak To Average Power Ratio(PAPR) in Orthogonal Frequency Division Multiplexing (OFDM) systems. OFDM system using multirate building blocks are used. OFDM is a particular case of transmultiplexer where the rectangular pulse is taken as the prototype filter in

analysis and synthesis filter banks. But because of rectangular window for prototype filter, the transmit and receive filters suffer from poor frequency responses. The bandwidth efficiency can be achieved by using non-rectangular windows for pulse shaping in such a manner that the cascade of transmit and receive filters meet the Nyquist criterion[10, 14, 29] . Nonrectangular windows have been proposed in [15, 29] to improve the spectral roll-off of the transmitted signals.Nyquist pulse shaping for multicarrier modulation is explained in[16, 17]. A new algorithm described in[18] is used to design the transmit and receive filters which satisfy Nyquist criterion.The filter so designed is used as an interpolating filter in an OFDM system to reduce PAPR .

1.2 Outline of the thesis

1.2.1 Multirate Systems and Filter Banks (Chapter 2)

In this chapter, we present a brief overview of multirate systems and some useful identities. Filter banks is dealt with significant detail. The chapter also deals with the interpretation of multirate systems as transmultiplexers and their significance in digital communication[32].

1.2.2 OFDM and Filter Bank Based Multicarrier ModulationSystems (Chapter 3)

This chapter starts with revisiting the fundamental concepts of OFDM.OFDM in terms of filter banks is explained. The chapter also addresses the issues associated with OFDM systems and introduces alternative approach to get over these

problems.

1.2.3 PAPR Reduction Methods and Pulse Shaping (Chapter 4)

This chapter defines the term PAPR and also presents various PAPR reduction methods for an OFDM system.It also describes the proposed method used to reduce PAPR in OFDM system which is based on pulse shaping.An algorithm is described which is used to design a pulse shaping filter known as Square Root Nyquist (M) Filter[18]

1.2.4 Discussion on Simulation Results (Chapter 5)

The simulations carried out at various steps in this journey are consolidated in this chapter.

1.3 Notations

Throughout the thesis, boldface letters are used for matrices and vectors. Lowercase letters are used for discrete sequences, while uppercase letter are used for Fourier and z-transforms. Superscripts (*) and (^{T}) denote the complex conjugate and transpose of a matrix (or vector) respectively, while superscript dagger (†) denotes the conjugate transpose. The identity matrix of size $N\ X\ N$ is denoted by $\mathbf{I}_N$. In the time domain the decimated and expanded sequences are denoted by

$[x(n)]_{\downarrow M}$ and $[x(n)]_{\uparrow M}$ respectively. $\mathbf{F}(z)$ and $\mathbf{H}(z)$ stand for synthesis and analysis filter banks respectively, while $F_k(z)$ and $H_k(z)$ denote the individual synthesis and analysis filters.

Chapter 2

Multirate Systems and Filter Banks

Multirate systems span an extensive range of applications in many areas of signal processing including filter bank theory, transmultiplexers, perfect reconstruction systems[1]-[6]. Unlike the single-rate system, the sample spacing in a multirate systemcan vary from point to point.This often results in more efficient processing of signals because the sampling rates at various internal points can be kept as small as possible. Multirate building blocks are the essential ingredients in many modern communication systems such as Orthogonal Frequency Division Multiplexing(OFDM)[7]-[10] .The use of multiple sampling rate offers many advantages such as reduced computational complexity, reduced transmission rate and reduced storage requirement based on the application[13]. This chapter presents a brief overview of multirate systems and some useful identities. Filter banks is dealt with significant details. The chapter also explains the use of multirate systems as transmultiplexers and their significance in digital communication.

2.1 Fundamental concepts

2.1.1 Basic building blocks

Multirate systems consist of two primary building blocks namely Interpolator and Decimator, which operate on a discrete time signal $x(n)$ to produce the output $y(n)$.These blocks are linear and time varying.

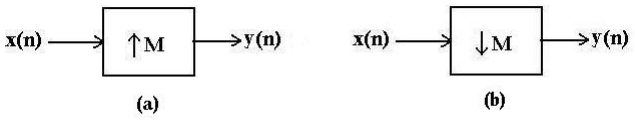

FIGURE 2.1: The basic multirate building blocks

2.1.1.1 Interpolator

An M-fold interpolator, indicated by Fig. 2.1(a), stretches the signal $x(n)$ by inserting $M-1$ zeros between its adjacent samples. The input-output relation for an interpolator with factor M is defined as:

$$y(n) = \begin{cases} x(\frac{n}{M}) & n \ = \ mul \ of \ M \\ 0 & otherwise \end{cases} \tag{2.1}$$

which in transform domain takes the form

$$Y(z) = X(Z^M) \ or \ Y(e^{j\omega}) \ = \ X(e^{j\omega M}) \tag{2.2}$$

$Y(e^{j\omega})$ is a M-fold compressed version of $X(e^{j\omega})$. Since $X(e^{j\omega})$ is periodic with 2π, the function $Y(e^{j\omega})$ has a period of $\frac{2\pi}{M}$. As a result of the operation of expanding, multiple copies of the basic spectrum come into the picture. The effect, termed as

imaging, is demonstrated in Fig. 2.2. The images can be eliminated by applying a low pass filter with cut-off frequency $\approx \frac{\pi}{M}$ preceded by the interpolator called as antiimaging filter.

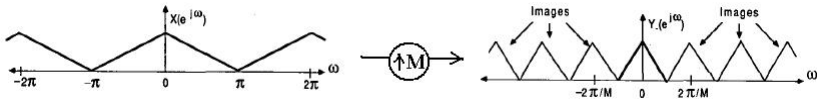

FIGURE 2.2: Transform domain effect of interpolator

2.1.1.2 Decimator

The output $y(n)$ of a decimator (indicated in Fig. 2.1(b)) is the compressed version of the input $x(n)$. The input-output relation for M-fold decimator is given by:

$$y(n) = x(Mn) \tag{2.3}$$

The transform domain analysis of the decimator produces the output as:

$$Y(Z) \;=\; \frac{1}{M}\sum_{k=0}^{M-1} X(Z^{\frac{1}{M}}W^k) \tag{2.4}$$

which alternatively in frequency variable can be expressed as:

$$Y(e^{j\omega}) \;=\; \frac{1}{M}\sum_{k=0}^{M-1} X(e^{\frac{j(\omega-2\pi k)}{M}}) \tag{2.5}$$

(2.5) shows that $Y(e^{j\omega})$ is a sum of M uniformly shifted versions of an M-fold stretched version of $X(e^{j\omega})$. Only those samples of $x(n)$ which occur at time equal to multiples of M are retained by the decimator.The aliases induced by decimator cause the loss of information because of the possible overlap of the shifted versions of $Y(e^j\omega)$, which is presented in Fig. 2.3. A low pass filter called antialiasing filter

with cut-off frequency $\approx \frac{\pi}{M}$ followed by the decimator band limits the signal and reduce the aliasing effect.

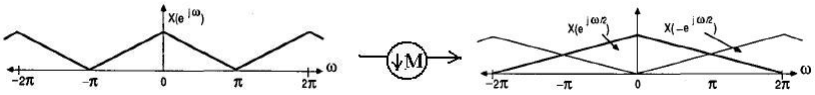

FIGURE 2.3: Demonstration of aliasing effect for M=2

2.1.2 Multirate identities and polyphase structure

Polyphase representation of signals plays a significant role in multirate signal processing by facilitating considerable simplifications of theoretical results as well as efficient implementation of multirate system.With great efficiency we can construct a filter bank at the cost of one single filter.The cost of filter bank is equal to the cost of prototype filter plus the IDFT computational cost.

2.1.2.1 The noble identities

Fig. 2.4(a) shows a decimator followed by a transfer function $G(z)$. It can be proved, based on (2.4) that this cascade is equivalent to the one in Fig. 2.4(b) provided $G(z)$ is a rational transfer function. In a similar manner, the two cascades of Fig. 2.4(c) and Fig. 2.4(d) are equivalent, subject to the same constraint. These are called *noble identities* and are highly important in all applications for efficient implementation of filters and filter banks.

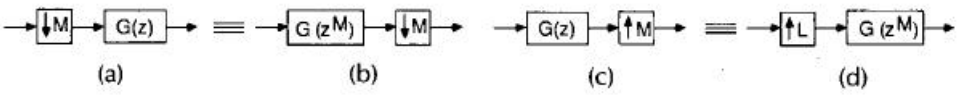

FIGURE 2.4: Noble identities for multirate systems

2.1.2.2 Polyphase representation

Consider an LTI system with a transfer function $H(z) = \sum_{n=-\infty}^{\infty} h(n)z^{-n}$ and suppose we are given an integer M. We can decompose $H(z)$ as

$$H(z) = \sum_{k=0}^{M-1} z^{-k} E_k(z^M) \quad (Type\ 1\ decomposition) \tag{2.6}$$

where

$$E_k(z) = \sum_{n=-\infty}^{\infty} e_k(n)z^{-n} = \sum_{n=-\infty}^{\infty} h(Mn+k)z^{-n} \qquad 0 \leq k \leq M-1 \tag{2.7}$$

(2.6) is called Type 1 polyphase representation (with respect to M) and $E_k(z)$ the polyphase components of $H(z)$.Type 1 polyphase decomposition is like dividing the impulse response $h(n)$ into M nonoverlapping group of samples $E_k(n)$,obtained from $h(n)$ by M fold decimation starting from sample k. The polyphase components work at M times lower sampling rate than the original signal. A variation of (2.6) is obtained if we decimate $h(n)$ starting from sample $-k$ for $0 \leq k \leq M-1$. This gives rise to Type 2 polyphase representation, where the components $R_k(z)$ are the permutations of $E_k(z)$ i.e. $R_k(z) = E_{M-1-k}(z)$.

$$H(z) = \sum_{k=0}^{M-1} z^{-(M-1-k)} R_k(z^M) \quad (Type\ 2\ decomposition) \tag{2.8}$$

2.2 Multirate filter banks

A digital filter bank is a collection of filters with either a common input or a summed output, as shown in Fig. 2.5. The analysis filter bank consisting of analysis filters $H_k(z)$ decomposes the signal into M consecutive subband signals

$x_k(n)$. On the other hand, the set of subband signals $y_k(n)$ is combined into one signal $\hat{x}(n)$ by the synthesis which is composed of synthesis filters $F_k(z)$.

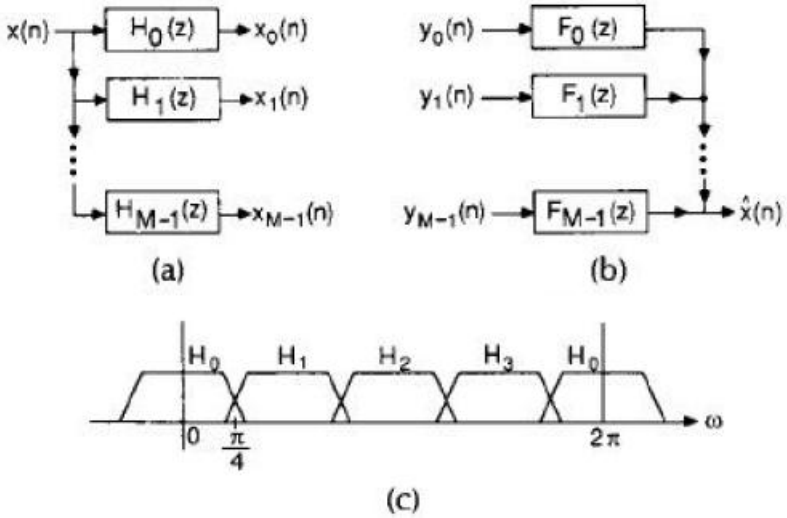

FIGURE 2.5: (a) Analysis filter bank (b) Synthesis filter bank (c) Typical response of uniform DFT filter bank for M=4

2.2.1 Uniform DFT filter banks

An analysis bank with M filters ($M > 1$) is said to be a uniform DFT filter bank if all the filters $H_k(z)$ are expressed as:

$$H_k(z) = H_0(zW^k),\ 0 \leq k \leq M-1 \tag{2.9}$$

The filter $H_o(z)$ is called the prototype filter. From the frequency domain transform of (2.9), it can be seen that $H_k(e^{j\omega}) = H_0(e^{j(\omega - \frac{2\pi k}{M})})$, which means that the frequency responses of $H_k(z)$ are uniformly shifted versions of $H_0(e^{j\omega})$. The response of 4-band DFT filter bank is demonstrated in Fig. 2.5(c).The filter order is proportional to M.However,by using polyphase decomposition DFT filter bank can be implemented in an efficient manner.Although the filter order increases as M increases but the number of computations per output sample is independent of

M using polyphase approach. Assuming that the prototype filter $H_0(z)$ has been written in the form of (2.6). The kth filter can now be expressed as

$$H_k(z) \; = H_0(zW^k) \; = \; \sum_{l=0}^{M-1} (z^{-1}W^{-k})^l E_l(z^M) \tag{2.10}$$

The output $X_k(z)$ of the analysis DFT bank is then given as

$$X_k(z) = \sum_{l=0}^{M-1} W^{-kl}\Big(z^{-1}E_l(z^M)X(z)\Big) \tag{2.11}$$

This shows that the M filters can be implemented by using the structure shown in Fig. 2.6. If $H(z)$ is FIR with order N, the implementation of polyphase components requires $N+1$ multiplications and $N-M+1$ additions.

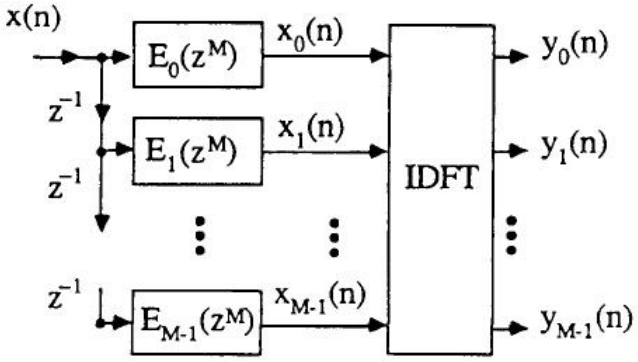

FIGURE 2.6: A uniform DFT analysis filter bank

The reverse arrangement of analysis and synthesis bank i.e. when the synthesis bank is followed by analysis DFT bank known as transmultiplexer(devices for converting between frequency division multiplexing(FDM) and time division multiplexing(TDM)),is used in modern communication systems i.e. Orthogonal Frequency Division Multiplexing (OFDM). OFDM is treated with more detail in the next chapter.

2.2.1.1 Polyphase implementations of two-channel structures

Suppose each of the analysis filter is decomposed as

$$H_k(z) = E_{k0}(z^2) + z^{-1}E_{k1}(z^2),\ \ k = 0, 1 \tag{2.12}$$

Similarly, the synthesis filters can be viewed as

$$F_k(z) = z^{-1}R_{0k}(z^2) + R_{1k}(z^2),\ \ k = 0, 1 \tag{2.13}$$

Equivalently, the analysis and synthesis filters can be collected in matrix form as

$$\begin{bmatrix} H_0(z) \\ H_1(z) \end{bmatrix} = \begin{bmatrix} E_{00}(z^2) & E_{01}(z^2) \\ E_{10}(z^2) & E_{11}(z^2) \end{bmatrix} . \begin{bmatrix} 1 \\ z^{-1} \end{bmatrix} \tag{2.14}$$

and

$$\begin{bmatrix} F_0(z) & F_1(z) \end{bmatrix} = \begin{bmatrix} z^{-1} & 1 \end{bmatrix} . \begin{bmatrix} R_{00}(z^2) & R_{01}(z^2) \\ R_{10}(z^2) & R_{11}(z^2) \end{bmatrix} . \tag{2.15}$$

Using the matrix form, Fig. 2.7 can be redrawn as in the form of Fig. 2.8(a), where $\mathbf{E}(z) = [E_{kn}^{(z)}], 0 \leq k, n \leq M-1$, and $\mathbf{R}(z) = [R_{kn}^{(z)}], 0 \leq k, n \leq M-1$. Now the decimator blocks of Fig. 2.8(a) can be moved prior to $\mathbf{E}(z)$ using noble identity of Fig. 2.4(a,b). Similarly, the interpolators can be moved after $\mathbf{R}(z)$ using noble identity of Fig. 2.4(c,d). The resulting structure can be drawn as in Fig. 2.8(b), where $\mathbf{P}(z) = \mathbf{R}(z)\mathbf{E}(z)$. It can now be concluded that if the filters $H_k(z)$ and $F_k(z)$ are such that

$$\mathbf{R}(z) = \mathbf{E}^{-1}(z) \tag{2.16}$$

then the system of Fig. 2.8(b) reduces to that presented in Fig. 2.9, which is a perfect reconstruction system.

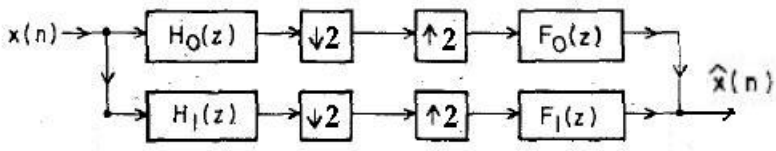

FIGURE 2.7: Two-channel QMF bank

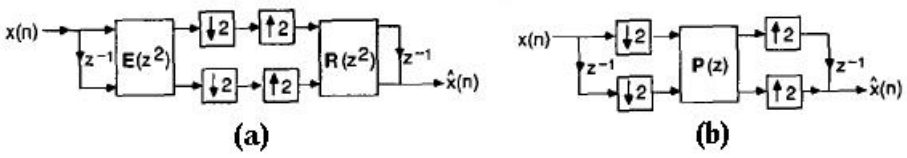

FIGURE 2.8: (a)Redrawing the two-channel QMF bank (b)$P(z) = R(z)E(z)$

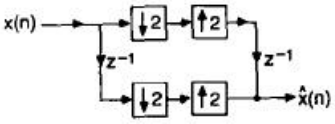

FIGURE 2.9: Trivial perfect reconstruction system

2.2.1.2 Polyphase implementation of M-channel structures

The interpretation of the two-channel structure enables the extension of this idea to for M channels. Taking the polyphase representation of the M-channel QMF bank, Fig. 2.10 can be redrawn as in Fig. 2.11 which after further simplification takes the form of Fig. 2.12(a).

The analysis filters $H_k(z)$ can be expressed in the form

$$H_k(z) \;=\; \sum_{l=0}^{M-1} z^{-l} E_{kl}(z^M) \;\; (Type\ 1\ polyphase) \tag{2.17}$$

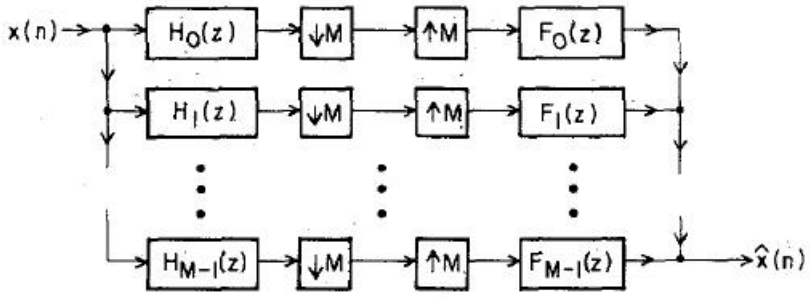

FIGURE 2.10: M-channel QMF bank

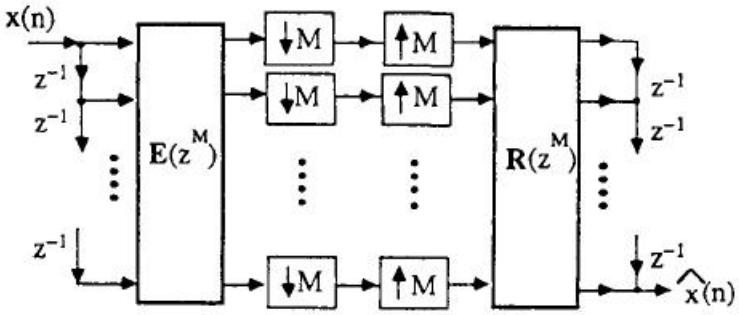

FIGURE 2.11: Redrawing of M-channel QMF bank with polyphase matrices

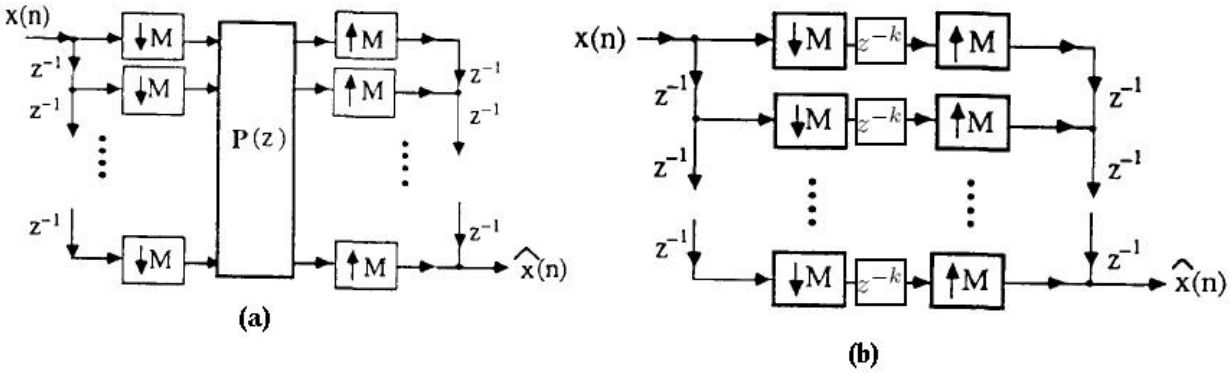

FIGURE 2.12: (a)$P(z) = R(z)E(z)$ (b) A structure equivalent to (a) when $E(z)$ is lossless

which can be rewritten as

$$\begin{bmatrix} H_0(z) \\ \vdots \\ H_{M-1}(z) \end{bmatrix} = \begin{bmatrix} E_{00}(z^M) & E_{01}(z^M) & \dots & E_{0,M-1}(z^M) \\ \vdots & \vdots & \vdots & \vdots \\ E_{M-1,0}(z^M) & E_{M-1,1}(z^M) & \dots & E_{M-1,M-1}(z^M) \end{bmatrix} \cdot \begin{bmatrix} 1 \\ z^{-1} \\ \vdots \\ z^{(M-1)} \end{bmatrix} \tag{2.18}$$

Identically, the et of synthesis filters can be expressed as

$$F_k(z) = \sum_{l=0}^{M-1} z^{-(M-1-l)} R_{kl}(z^M) \quad (Type\ 2\ decomposition) \tag{2.19}$$

which in matrix notation takes the form

$$\begin{bmatrix} F_0(z) & \dots & F_{M-1}(z) \end{bmatrix} = \begin{bmatrix} z^{-(M-1)} & z^{-(M-2)} & \dots & 1 \end{bmatrix} \cdot$$

$$\begin{bmatrix} R_{00}(z^M) & R_{01}(z^M) & \dots & R_{0,M-1}(z^M) \\ \vdots & \vdots & \vdots & \vdots \\ R_{M-1,0}(z^M) & R_{M-1,1}(z^M) & \dots & R_{M-1,M-1}(z^M) \end{bmatrix} \tag{2.20}$$

If the analysis matrix $\mathbf{E}(z)$ is lossless, then so will be $\mathbf{R}(z)$. So chosen $\mathbf{E}(z)$ causes $\mathbf{P}(z)$ in Fig. 2.12(b) to take the form $\mathbf{P}(z) = cz^{-k}\mathbf{I}$, which ensures perfect reconstruction. Tersely stating, a QMF bank gives rise to perfect reconstruction if its $\mathbf{P}(z)$ matrix is of the form $cz^{-k}\mathbf{I}$. The reconstructed signal is then given by $\hat{x}(n) = cx(n - kM - M + 1)$.

2.3 Multirate systems and digital communications

Fig. 2.13 shows the block diagram of the general communication system. The main goal of the system is to ensure that the received symbol $\hat{x}(n)$ resembles the original signal $x(n)$ under some criterion.When the analysis and synthesis bank filters of QMF bank change their position we get a widely accepted structure in

modern communication system known as *transmultiplexer* where synthesis bank follows the analysis bank and is used to implement OFDM system .

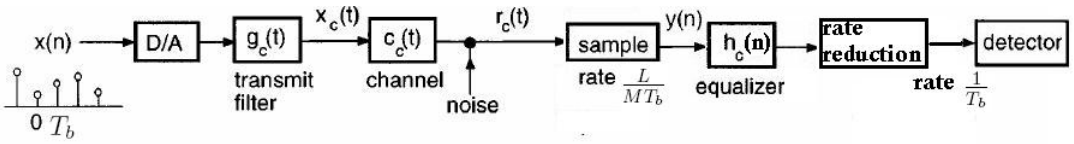

FIGURE 2.13: Digital communication system

2.3.1 Transmultiplexers (TMUX)

To define formally, a transmultiplexer is a multi-input, multi-output, multirate structure which is exactly opposite to that of M-channel QMF bank. The critical time sampling in QMF banks corresponds to critical frequency sampling in TMUX. The objective of removing the aliases in QMF bank mounts to the one to eliminate the cross talk in TMUX [7]. The operation of the TMUX system indicated in Fig. 2.14, the M input signals x_i are first upsampled by M. The obtained signals are then interpolated by $F_i(z)$ and summed to form the channel signal $y(n)$. At the receiver y is filtered by $H_k(z)$ and subsampled by M to form the reconstructed signals $\hat{x}_i$.

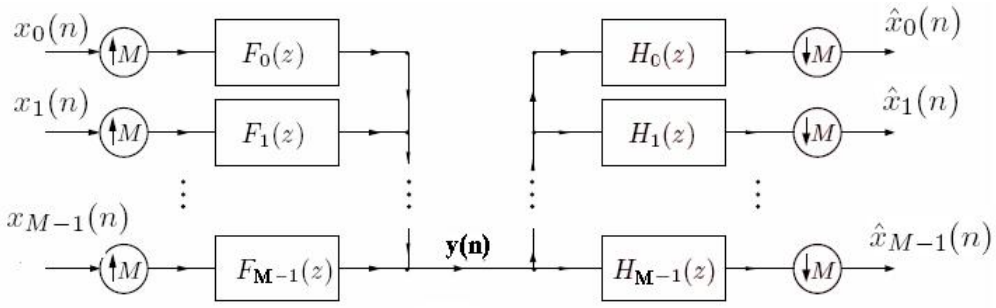

FIGURE 2.14: Transmultiplexer structure drawn in terms of filer bank notations

Using (2.2) and (2.4), it can be verified that the ith reconstructed signal can be expressed as

$$\hat{X}_i(z) = \frac{1}{M}\sum_{k=0}^{M-1} H_i(z^{\frac{1}{M}}W^k).\sum_{j=0}^{M-1} F_j(z^{\frac{1}{M}}W^k)X_j(z) \tag{2.21}$$

Substituting z^M for z in (2.21) (which means that all transfer functions are now expressed at the channel sampling frequency), and using matrix notation, (2.21) can be written as

$$\hat{\mathbf{x}}(z^M) = \frac{1}{M}[\mathbf{H}_m(z)]^T.\mathbf{F}_m(z).\mathbf{x}(z^M) \tag{2.22}$$

where

$$\mathbf{x}(z^M) = \begin{bmatrix} X_0(z^M) & X_1(z^M) & \dots & X_{M-1}(z^M) \end{bmatrix}^T \tag{2.23}$$

$$\mathbf{H}_m(z) = \begin{bmatrix} \mathbf{h}(z) & \mathbf{h}(Wz) & \dots & \mathbf{h}(W^{M-1}z) \end{bmatrix}^T \tag{2.24}$$

with

$$\mathbf{h}(z) = \begin{bmatrix} H_0(z) & H_1(z) & \dots & H_{M-1}(z) \end{bmatrix}^T \tag{2.25}$$

$$\hat{\mathbf{x}}(z^M) = \begin{bmatrix} \hat{X}_0(z^M) & \hat{X}_1(z^M) & \dots & \hat{X}_{M-1}(z^M) \end{bmatrix} \tag{2.26}$$

(2.22) signifies that crosstalk gets canceled iff

$$[\mathbf{H}_m(z)]^T.\mathbf{F}_m(z) = c\mathbf{I} \tag{2.27}$$

for some constant c. The condition (2.27) is similar to that for perfect reconstruction in case of QMF bank.

2.3.2 TMUX in terms of polyphase matrices

The use of polyphase decomposition adds further insight into the operation of TMUX. The analysis and synthesis banks of Fig. 2.14 can be redrawn in terms of polyphase matrices $\mathbf{E}(z)$ and $\mathbf{R}(z)$ as shown in Fig. 2.15. The figure is obtained by usnig noble identites and thus shifting the upsampling blocks post to $\mathbf{R}(z)$ and moving the downsampler prior to $\mathbf{E}(z)$.

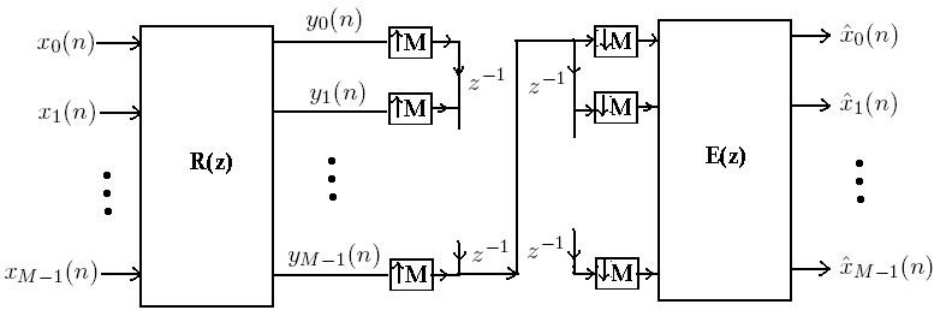

FIGURE 2.15: Equivalent structure for the TMUX in terms of polyphase matrices

If the prototype filter is of the form

$$F_0(z) = \begin{bmatrix} 1 & z^{-1} & \dots & z^{-(M-1)} \end{bmatrix} \tag{2.28}$$

then the TMUX structure reduces to the widely accepted technique OFDM.

OFDM have achieved great success and popularity in both wired and wireless transmission. But OFDM transceiver suffers from poor frequency characteristics and also high Peak to average Power Ratio(PAPR) because the transmitted symbol consists of sum of signals of different amplitude and also because of the use of rectangular window for pulse shaping. The spectral roll-off and PAPR of the transmitted signal can be improved if the rectangular pulse shaping filters are

replaced by the non-rectangular ones which meet certain constraints. The need for bandwidth efficient systems sets a strong foundation to step toward the filters satisfying Nyquist property which, if designed properly, could prove a good alternative in the direction of ISI mitigation and reduction in PAPR. The next chapter focuses on the impact of wireless channel and various steps to effectively communicate the data over it.

Chapter 3

OFDM and Filter Bank based Multicarrier Systems

Multicarrier systems, especially OFDM, are successfully established in many communications standards because of their robustness against narrow-band co- channel interference and ISI,efficient implementation and less sensitive to sample timing offsets. Looking from the mutirate viewpoint, these systems are essentially the transmultiplexers (TMUX) with different prototype filters.

This chapter starts with revisiting the fundamental concepts of OFDM[33] in Section 3.1. A slightly different approach to capture the underlying characteristics of OFDM is presented in Section 3.2 based on multirate system.Advantages and disadvantages of OFDM is discussed in Section 3.3 and 3.4 Section 3.3.Section 3.5 introduces approach to get over these problems.

3.1 Overview of OFDM system

OFDM is a multicarrier modulation scheme which converts a high rate data streams into a number of low rate streams that are transmitted over parallel,narrowband channels simultaneously. The sub carriers are orthogonal to each other. Orthogonality is achieved by spacing two adjacent sub carriers by $1/T_s$ where T_s is the symbol period.i.e

$$f_c = \frac{1}{T_s} \tag{3.1}$$

Different modulation schemes like QAM,QPSK,BPSK etc can be used for different sub carriers. The k_th subcarrier then can be given as

$$c_k(t) = \begin{cases} \mathrm{e}^{j2\pi f_c kt} & 0 \leq t \leq T_s \\ 0 & otherwise \end{cases} \tag{3.2}$$

the frequency of k_th subcarrier can be expressed as

$$f_k = kf_c \tag{3.3}$$

The orthogonality condition can be symbolized as

$$\int_0^{T_b} c_k(t)c_p^*(t) = \begin{cases} T_b & k = p \\ 0 & otherwise \end{cases} \tag{3.4}$$

In other words, two subcarriers are said to be orthogonal if their inner product is zero unless both are same.The orthogonality property of the subcarriers allows them to overlap, yet to carry the data separately. This serves as the principal behind OFDM. The systems exploiting the orthogonality condition enjoy the benefit of the spectral efficiency as demonstrated in Fig. 4.1.

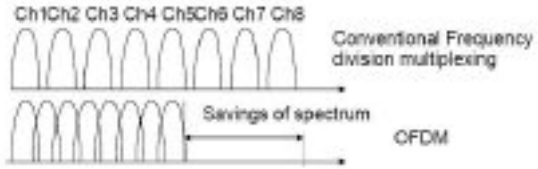

FIGURE 3.1: Comparison of spectral efficiency of OFDM with that of conventional FDM

3.1.1 OFDM Modulator

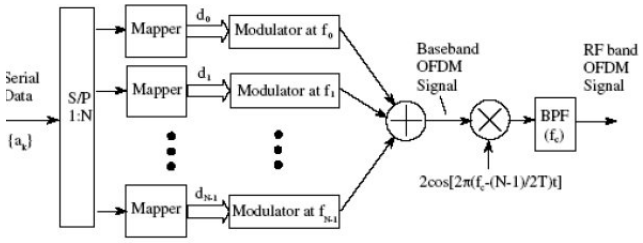

FIGURE 3.2: OFDM modulator

OFDM modulator is shown in Fig3.2. Serial data bits are converted to N data streams by 1:N serial to parallel converter. In the mapper block bits in each data stream are combined into k tuples and each of k tuple is mapped to a symbol represented by a complex number

$$d_i = A_i exp(j\Phi_i) = I_i + jQ_i \quad i = 0, 1, ..., N-1 \tag{3.5}$$

where

$$I_i = A_i \cos \Phi_i \tag{3.6}$$

$$Q_i = A_i \sin \Phi_i \tag{3.7}$$

Each of the symbol is modulated using different subcarriers . We can use different modulation scheme for different sub carriers. There are N modulators for N sub carriers. Adder combines all the symbols generates a baseband OFDM signal. For a band pass OFDM signal an adder is followed by an RF mixer with a reference

frequency of $f_c = f_c - N - 1/2T$ and a bandpass filter which is centered at f_c and hence rejects the lower sideband of mixer output.

3.1.2 Demodulator

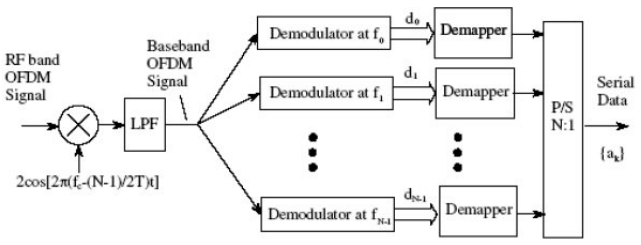

FIGURE 3.3: OFDM Demodulator

OFDM demodulator is shown in Fig3.3 Bandpass OFDM is first converted to baseband OFDM by a down converter before demodulation is done. For N subcarriers we have N demodulators. Type of demodulator is based on the type of modulation used. Each demodulator basically consist of local oscillator,multipliers integrator threshold detector. Grouped bits are despread in demapper block and is converted to a serial data stream using parallel to serial converter.

3.1.2.1 Disadvantages:

- As N increases the number of components i.e. modulator demodulator also increases and hence the system becomes complex.
- To maintain orthogonality between subcarriers certain requirements are imposed on filter frequency response which is difficult to maintain.

3.1.3 DFT Based Digital OFDM

The band pass OFDM signal is given as:

$$s(t) = Re\{(\sum_{i=0}^{N-1} d_i exp(j2\pi \frac{i}{T}t) exp[j2\pi(f_c - \frac{N-1}{2T})t]\} \; 0 \leq t \leq T \tag{3.8}$$

where

$$d_i = A_i exp(j\phi_i) = I_i + jQ_i \tag{3.9}$$

The complex envelope of band pass OFDM w.r.t lower carrier frequency is:

$$\tilde{s}(t) = \sum_{i=0}^{N-1} d_i exp(j2\pi \frac{i}{T}t) \; 0 \leq t \leq T \tag{3.10}$$

Baseband OFDM signal is given as:

$$s(t) = Re[\sum_{i=0}^{N-1} d_i exp(j2\pi \frac{i}{T}t)] = Re[\tilde{s}(t)] \; 0 \leq t \leq T \tag{3.11}$$

IDFT is obtained by sampling the complex envelope $s(t)$ with a sampling period of $t = T/N$, and adding a normalizing factor $1/N$, Thus OFDM signal can be generated by IDFT.For demodulation we use DFT.

$$s_n = \frac{1}{N} \sum_{i=0}^{N-1} d_i exp(j2\pi \frac{in}{N}) \quad n = 0, 1, 2, 3, ..., N-1 \tag{3.12}$$

The above method suffers from aliasing as shown in Fig3.4 because the sampling frequency is only N/T however for proper sampling it should be $2N/T$. To remove aliasing[20]Fig3.5 we append N zeroes in data set $\{di\}$ to make it $2N$

$$d_0, d_1, ..., d_N - 1, \underbrace{0, 0, ..., 0}_{NZeros}$$

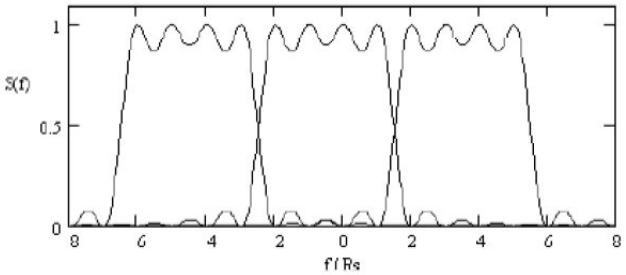

FIGURE 3.4: PSD of OFDM signal for four subcarriers without virtual carriers

and a $2N$ point IDFT is used to generate OFDM signal and N point DFT to demodulate the signal. Only N point DFT pair is used to generate $2N$ point DFT but the speed of the processors is double that of the symbol rate. In the modulator to obtain real and imaginary OFDM signal the complex data is passed through N point IDFT twice. In demodulator also real and imaginary components are passed to N point DFT twice to generate the original signal. Aliasing can also be reduced

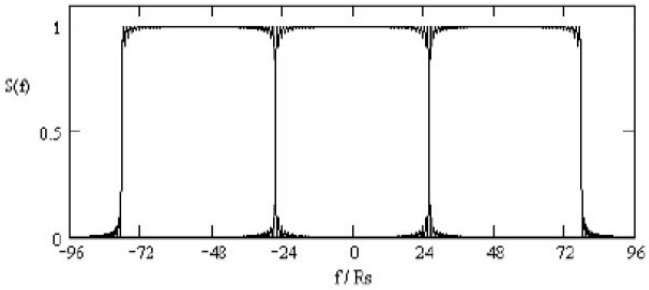

FIGURE 3.5: PSD of OFDM signal for 52 subcarriers without virtual subcarriers

by over sampling the data[33] as shown in Fig3.6 . It is done by appending zeroes to the data set. If L zeroes are appended then $L/2$ are appended before the data set and $L/2$ after the data set.

$$\underbrace{0, 0, ..., 0}_{L/2zeros}, d_{-\frac{N}{2}}, d_{-\frac{N}{2}+1}, ..., d_{\frac{N}{2}-1}, \underbrace{0, 0, ...0}_{L/2zeros}$$

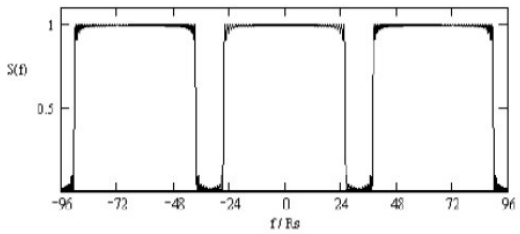

FIGURE 3.6: PSD of OFDM signal for 52 subcarriers plus six virtual subcarriers on each side

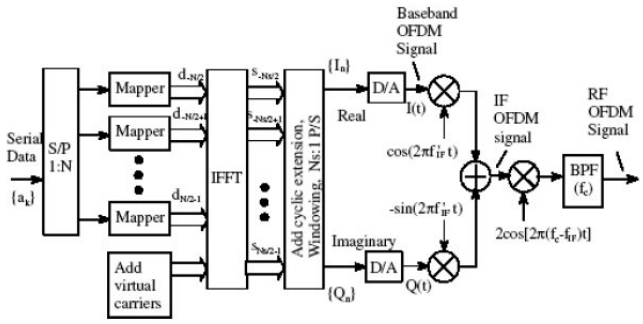

FIGURE 3.7: IFFT based modulator

3.1.4 IFFT Based Modulator

As shown in Fig3.7.serial data is converted to symbol $\{d_i\}_{i=-\frac{N}{2}}^{\frac{N}{2}-1}$ using serial to parallel converter and bits to symbol mapper. To avoid aliasing zeroes are added to the data set and the new data set has size N_s. The IFFT block transforms $\{d_i\}_{i=-\frac{N_s}{2}}^{\frac{N_s}{2}-1}$ into complex time domain samples $\{s'_n\}_{n=-\frac{N_s}{2}}^{\frac{N_s}{2}-1}$

$$s'_n = \frac{1}{N}\sum_{i=-\frac{N}{2}}^{\frac{N}{2}-1} d_i exp(j2\pi\frac{in}{N}) \quad n = -\frac{N}{2}, -\frac{N}{2}+1, ..., \frac{N}{2}-1 \tag{3.13}$$

The parallel to serial converter separates the complex signal into I-Q channel ie

$$I_n = \frac{1}{N}\sum_{i=-\frac{N}{2}}^{\frac{N}{2}-1} A_i \cos(2\pi\frac{in}{N} + \phi_i) \quad n = -\frac{N}{2}, -\frac{N}{2}+1, ..., \frac{N}{2}-1 \tag{3.14}$$

$$Q_n = \frac{1}{N}\sum_{i=-\frac{N}{2}}^{\frac{N}{2}-1} A_i \sin(2\pi\frac{in}{N} + \phi_i) \quad n = -\frac{N}{2}, -\frac{N}{2}+1, ..., \frac{N}{2}-1 \tag{3.15}$$

Cyclic extension is done to avoid ISI windowing is done to remove sidelobes. The D/A converter converts the digital signal into continuous time domain signal $I(t)$ and $Q(t)$.

$$I(t) = \frac{1}{N}\sum_{i=-\frac{N}{2}}^{\frac{N}{2}-1} A_i \cos(2\pi\frac{i}{T} + \phi_i) \quad -\frac{T}{2} \leq t \leq \frac{T}{2} \tag{3.16}$$

$$Q(t) = \frac{1}{N}\sum_{i=-\frac{N}{2}}^{\frac{N}{2}-1} A_i \sin(2\pi\frac{i}{T} + \phi_i) \quad -\frac{T}{2} \leq t \leq \frac{T}{2} \tag{3.17}$$

To generate bandpass OFDM $I(t)$ and $Q(t)$ are further modulated to IF carrier frequency $f'_{IF} = f_{IF} + \frac{1}{2T}$ then an up conversion is used to shift IF OFDM signal to RF band centered at f_c. BPF is centered at f_c has bandwidth $N + 1/T$ to allow desired term and reject the term having center frequency $f_c - 2f_{IF}$

3.1.5 Demodulator

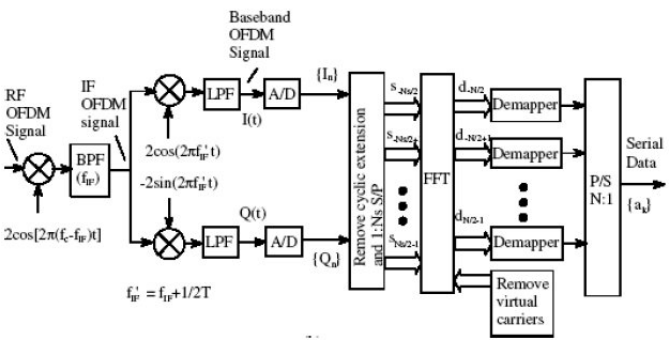

FIGURE 3.8: FFT based demodulator

FFT based demodulator is shown in Fig3.8.The RF OFDM signal is first down converted to IF band and IF OFDM signal is demodulated to baseband OFDM $I(t)$ and $Q(t)$. The A/D converter converts the continuous time signal into digital signal I_n and Q_n . The two samples are combined in S/P block and the cyclic

extension is removed. The FFT block converts $\{s'_n\}_{n=-\frac{N_s}{2}}^{\frac{N_s}{2}-1}$ to $\{d_i\}_{i=-\frac{N_s}{2}}^{\frac{N_s}{2}-1}$

$$d_i = \sum_{n=-\frac{N}{2}}^{\frac{N}{2}-1} s'_n exp(-j2\pi\frac{in}{N}) \quad n = -\frac{N}{2}, -\frac{N}{2}+1, ..., \frac{N}{2}-1 \tag{3.18}$$

The virtual carriers are removed and the demapper block demap the signal back to binary data stream. Noise effects are removed by using threshold detector in demapper block. The P/S converter converts the data stream into serial bits. Advantage:

- Complexity is reduced.N analog modulator and demodulator block is replaced by single IFFT/FFT block

3.2 OFDM using multirate systems

As detailed in Chapter 2, multirate systems play a significant role in communications systems in different forms, be it a TMUX, or fractional biorthgonal partners, or a channel precoder. Rearranging the blocks of Fig. 2.14 of Chapter 2 and drawing the synthesis part in a compact form in Fig. 3.9 represents the multiplexing unit of OFDM system. The blocking and unblocking operations are depicted in Fig. 3.10. The IDFT block of Fig. 3.9 generates M orthogonal subcarriers which are modulated by the data block x_k. By comparing Fig. 3.9 with Fig. 2.14 of Chapter 2, it can be easily interpreted that OFDM is a specific case of TMUX where the prototype filter $F_0(z)$ is selected as a rectangular window of length M, and rest of the filters in the filter bank are yielded by multiplying $F_0(z)$ with IDFT matrix. Following the similar track, the connection can be observed between the analysis part of TMUX and the demultiplexing mechanism of OFDM.

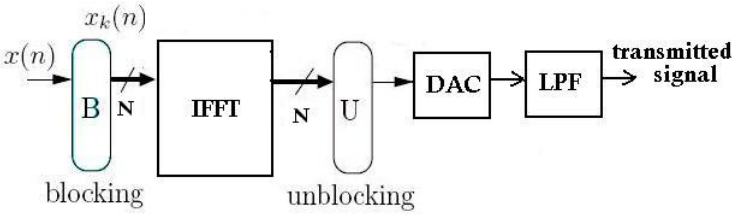

FIGURE 3.9: Multiplexing operation of OFDM regarded as synthesis filter bank of TMUX

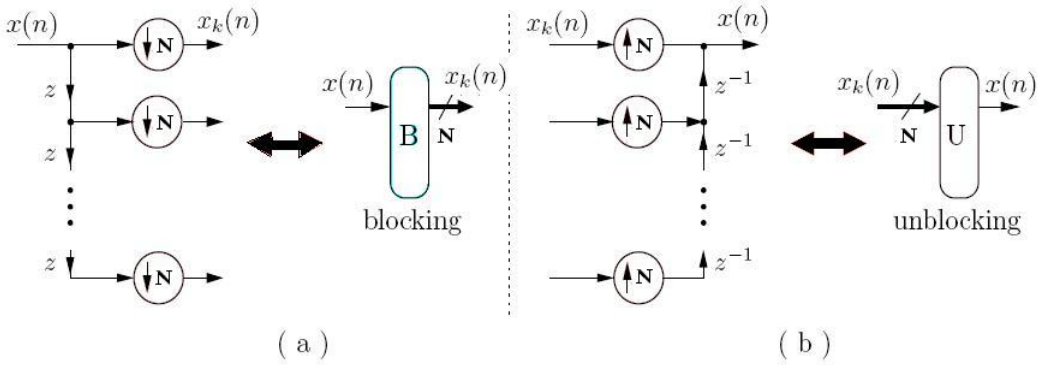

FIGURE 3.10: Notations: (a)Blocking and (b)Unblocking operations

3.3 Advantages of OFDM System

OFDM is highly used multicarrier modulation scheme in modern communication system due to follwing reasons:

- Makes efficient use of the spectrum by allowing spectral overlap.
- By dividing the channel into narrowband flat fading sub channels,OFDM is more resistant to frequency selective fading than single carrier systems.
- Robust against ISI caused by multipath propagation.
- Using adequate channel coding and interleaving one can recover symbols lost due to frequency selectivity of the channel.
- Channel equalization becomes simpler than by using adaptive equalization techniques with single carrier systems.

- OFDM can be easily implemented using IDFT/DFT pair.
- OFDM is less sensitive to sample timing offsets than single carrier systems.
- OFDM provides good protection against cochannel interference and impulsive parasitic noise.

3.4 Disadvantages of OFDM system

- The use of rectangular window as a pulse shaping filter, the transmit and receive filters suffer from poor frequency responses. The stopband attenuation is only 13 dB, and it decays at a rate of $\frac{1}{f}$ only [10]. It is desirable to have transmitters which have small out of band energy in many wireless communications applications. The required ideal bandwidth efficiency can be achieved by using non-rectangular windows for pulse shaping in such a manner that the cascade of transmit and receive filters meets the Nyquist criterion [16].
- OFDM system has high Peak to Average Power Ratio (PAPR). A comparison at the basis of the achievable data rates shows that OFDM is able to transmit $Mlog_2(\mathcal{M}_O)$ bits per symbol, whereas the TMUX transmits $(M+M_{cp})log_2(\mathcal{M}_T)$ bit per symbol, where $\mathcal{M}_O$ resp. $\mathcal{M}_T$ denote the modulation alphabets for OFDM resp. Root Raised Cosine-TMUX. If 25% cyclic prefix is assumed, i.e. $\frac{M_{cp}}{M} = \frac{1}{3}$, 256QAM resp. 16QAM is necessary for OFDM against 64QAM resp. 8QAM for a TMUX without CP. This means that more transmit power is necessary for OFDM in order to get the same (uncoded) bit error rates for the higher modulation schemes [9].
- OFDM system are sensitive to Doppler shift and frequency offset

3.5 What is the solution

Spectral characteristic can be improved by using non rectangular windows which satisfy the Nyquist criterion.Many pulse shaping filters have been proposed in [29] which helps to improve frequency response.We have used a new algorithm given in [18] to design transmit and receive filters which satisfy Nyquist criterion known as Square Root Nyquist(M) filter.The algorithm is described in Chapter 4.The algorithm also provides the freedom to control the value PAPR in a desired manner which is the central theme of the thesis.The filter so designed is used as an interpolating filter for an OFDM system.The resulting system for the transmitter is drawn in Fig. 3.11. The

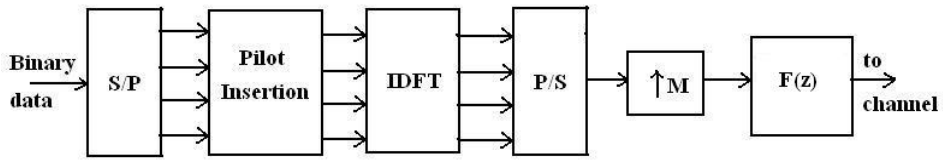

FIGURE 3.11: OFDM transmitting system with increased symbol rate

TMUX systems designed with the prototype filters $F_0(z)$ resp. $H_0(z)$ such that their cascade satisfies Nyquist property uses the algorithm described in Chapter 4 for designing of transmit and receive filters.But the system is not desirable in terms of computational complexity, so we use DFT filter bank and polyphase structures to reduce the complexity. When the number of channels is small, typically less than 20, the complexity is dominated by the filter bank. The complexity of the filter bank is proportional to the length of the pulse shaping filters and being able to use short filters could therefore significantly reduce the complexity. The delay is proportional to the pulse length which gives another motivation for short pulses[32].

Since in filter bank based multicarrier systems the basic symbol waveform is a Nyquist pulse overlapping with the previous and next symbol, so the orthogonality of subchannels is easily lost. Though the arbitrary scaling of the amplitudes does not affect the orthogonality, but the nonlinear phase response of channel does. One possible approach to eliminate the effects of nonlinear phase response is to use the ovesampled filter banks. Fig. 3.12 presents the model of such system, where $M \geq N$.

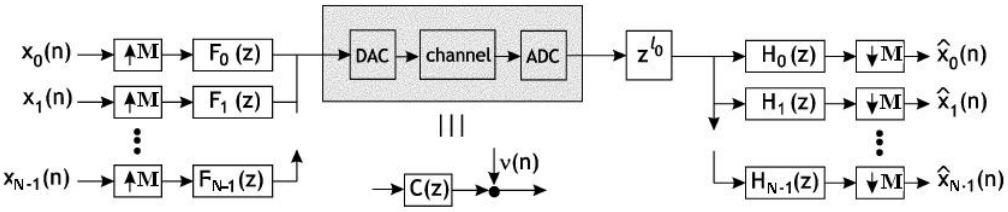

FIGURE 3.12: Filter bank transceiver

The system in Fig. 3.12 is LTI with the transfer function

$$T_{ij}(z) = [F_i(z)C(z)H_j(z)z^{l_0}]_{\downarrow M}$$

$$= \sum_{l=0}^{L} c(l)[F_i(z)H_j(z)z^{l_0-l}]_{\downarrow M} \tag{3.19}$$

where $L+1$ is the length of the channel. $[F_i(z)H_j(z)z^{l_0-l}]_{\downarrow M}$ can be expressed as

$$[F_i(z)H_j(z)z^{l_0-l}]_{\downarrow M} = \begin{cases} 1 & i = j \\ 0 & i \neq j \end{cases} \tag{3.20}$$

Therefore, the transfer function takes the form

$$T_{ij}(z) = \begin{cases} G_i & i = j \\ 0 & otherwise \end{cases} \tag{3.21}$$

where G_i is the cascade of $F(z)$ *and* $H(z)$, which satisfies Nyquist property according to (3.21). We design the filters $F(z) and H(z)$ by employing the algorithm described in [18].

In essence, the poor stopband attenuation of OFDM system can be overcome by using filter bank based multicarrier system. Also, the design algorithm for transmit and receive filters used here facilitates the control over PAPR.This filter is used as an interpolating filter to implement an OFDM system which results in reduction of PAPR.

Chapter 4

PAPR Reduction Methods and Pulse Shaping

High peak to average power is a major problem in OFDM system and can significantly degrade the power efficiency at the transmitter. The peak of the signal can be upto N times the average power(where N is the number of subcarriers) . High PAPR affects OFDM signal in 2 ways.Firstly, it generates high out of band noise.Secondly,nonlinearities of amplifier causes inband distortion of the signal resulting in higher bit error rates(BER).High PAPR leds to increase in dynamic range of amplifier as a resultof which cost of implementation increases.Minimising PAPR allows a higher average power to be transmitted for a fixed peak power. Proper shaping of transmitted pulse leads to decrease in PAPR value and also helps in reducing Inter Symbol Interference(ISI) .The basic objective of pulse shaping is the localization of signal in time-frequency plane i.e.the basic pulse shape should be well localized in time and its spectrum should be well localized as well. The pulse shape itself is chosen to ensure a bandlimited signal spectrum. The filters

$w(n)$ and $w1(n)$, used as transmit and receive filters respectively, should be selected such that their cascade meets Nyquist condition.

In this chapter we define PAPR and various PAPR reduction methods are discussed. Need for pulse shaping is also addressed.

4.1 Peak To Average Power Ratio

According to central limit theorem a linear combination of large number of independent random signals is approximated by Gaussian Distribution.Since in a typical OFDM system the value of N is large so the OFDM symbol can be approximated by a Gaussian distributed signal.This implies that some samples have a high probability of large peaks. To transmit a signal that has high peaks requires from the power amplifier in the transmitter to have a high signal span. Such amplifiers consume high power and are also costly. If we lower the average power of the signal then this will also lower the peaks that a power amplifier needs to handle. However reducing the average power of the signal will reduce the SNR at the receiver thus degrading performance. If we do not lower the average power of the amplifier input signal but we do not allow large peaks to pass through the amplifiers means we clip high signal peaks. This clipping introduces nonlinearities into the transmitted OFDM symbol. These nonlinearities cause an increase in bit error rate probabilities and also lead to higher out of band spectrum due to higher order harmonics.

4.2 Mathematical definition of PAPR

Mathematically, the PAPR for a given OFDM block can be written as[21]

$$PAPR(x[n]) = \frac{\max\limits_{0 \leq n \leq N-1} |x[n]|^2}{E\{x^2[n]\}} \tag{4.1}$$

where $\max\limits_{0 \leq n \leq N-1} |x[n]|^2$ denotes the maximum instantaneous power and $E\{x^2[n]\}$ denotes the average power of the signal. The peak level before and after the addition of the cyclic prefix will be same because the cyclic prefix is just a copy of a part of the original signal block. The peak power of the symbol will be the same and the average power of the symbol will not change either. This PAPR definition is also denoted as block or symbol PAPR. In opposite to that we can also define the sample PAPR as

$$PAPR(x[n_k]) = \frac{|x[n_k]|^2}{E\{x^2[n]\}} \tag{4.2}$$

where $|x[n_k]|^2$ represents the instantaneous power of the sample k and $E\{x^2[n]\}$ denotes average power of the OFDM block. In a practical system oversampled signals are considered and the PAPR of $x[n/L]$ can be easily computed. The peak power is defined as

$$max|x^m[n/L]|^2 = \frac{1}{N}|\sum_{k=0}^{N-1} X_k^m exp^{j2\pi kn/NL}|^2 \leq \frac{1}{N}[\sum_{k=0}^{N-1} max|X_k^m|]^2 \tag{4.3}$$

If we use the Parsevals relationship the average power can be computed as

$$E\{|x^m[n/L]|^2\} = \frac{1}{N}\sum_{k=0}^{N-1} E|X_k^m|^2 \tag{4.4}$$

Using above results the PAPR can be computed easily. Assuming the same signal constellation on all tones reveals that PAPR can be upper bounded by

$$PAPR\{x^m[n/L]\} \leq N\frac{max|X_k|^2}{E[|X_k|^2]} \tag{4.5}$$

where equality is achieved for example at $n = 0$ when all QAM subsymbols have the same phase, i.e.

$$arg\{X_0^m\} = arg\{X_k^m\}, \quad k = 1, ...N-1 \tag{4.6}$$

4.3 PAPR Reduction Methods

The PAPR is considered as one of the major problem in the multicarrier communication systems and a large number of efforts have been put to solve this problem. A number of PAPR reduction schemes have been proposed. Basically PAPR reduction schemes are categorized into 2 parts[21]: Transparent method and Non Transparent method

4.3.1 Transparent methods

In this method the receiver does not require knowledge about the method applied by the transmitter to reduce PAPR for detection process. Similarly, the receiver can use a method unknown to the transmitter. These methods can be easily implemented in existing standards without any changes to existing specifications. This thesis focuses on a transparent method.

4.3.1.1 Clipping

In this the amplitude of the OFDM signal is limited upto a certain threshold level. Signals having higher amplitude then the threshold level gets clipped off. As the number of signals having large amplitude is less clipping does not result in much of the performance degradation. Clipping causes re-growth of the signal peaks after the subsequent interpolation. To avoid the signal re-growth some techniques clip the signal after interpolation and then use a filter to reduce the resulting out-of-band spectral leakage. However the filters used in these techniques are complicated and computationally expensive. In addition they cause peak re-growth and result in significant distortion of the wanted signal[22] . The peak- windowing scheme presented in [28] is one of the clipping techniques that try to minimize the out of band distortion by using narrowband windows.

4.3.1.2 Tone Reservation

In the tone reservation method the orthogonality between the different subcarrier is exploited to generate the peak reduction signal. In the OFDM system not all subcarriers are used for data transmission. Some of them are reserved for the reduction signal. Due to the fact that all subcarrier are orthogonal the signal generated by the reserved tones does not disturb the data carrying tones. In the tone reservation method both transmitter and receiver know the set of data carrying subcarriers. The construction of the reduction signal can be done in different ways with different complexities[22, 24, 25]. Advantages of tone reservation include among other no side information and low complexity. Performance is dependent on pilot position and also there is small amount of data rate loss.

4.3.1.3 Active Constellation extension

The active constellation extension method proposed in is an extension of the tone injection method for PAPR reduction[22]. In this technique, some of the outer signal constellation points in the data block are dynamically extended towards the outside of original constellation such that the PAPR of data block is reduced. Here only the points at the constellation boundary have multiple representations and these points can be moved anywhere. The advantage with this method is that the decision regions for the receiver are not changing, so neither receivers nor the standard have to be changed. In systems that have very large constellations only a small part of the constellations is placed on the edges and there are fewer possibilities to move the points on the constellation boundaries, in these cases the reduction performance is low.It cannot be used for modulation schemes with large constellation size because the modifications results in increase in signal transmit power for the data block and hence cannot be applied for higher modulation shemes.

4.3.2 Non Transparent Methods

If the transmitter or the receiver incorporates a method to reduce PAPR that requires side information to be transmitted from one side to the other then it is called non transparent method. Majority of the PAPR reduction algorithms are included in this category.

4.3.2.1 Coding Schemes

Channel codes like parity check coding,cyclic coding,Rudin Shapiro coding are used for error control as well as to reduce peak amplitude of signals which results in low PAPR. Different coding schemes are presented in[26] that uses well-known block codes with constant-modulus constellations, such as QPSK and M-PSK for PAPR reduction purposes. The basic idea is that the block codes are used to remove some constellation combinations that produce large peaks and the encoded system will have smaller peaks then the uncoded system. One of the major drawbacks of this method is that it severely reduces data rate in order to achieve a good PAPR reduction.

4.3.2.2 Phase Optimization Techniques

It was observed that we will get large PAPR values when symbol phases in the subchannels are lined up in such a fashion that results in a constructive superposition forming a peak in the discrete time signal . By rotating the channel constellations properly the peaks can be reduced. The partial transmit sequence optimization scheme is such method[27]. In partial transmit sequence the data sequence is partitioned into several disjoint sequences combined linearly to form final sequence for IDFT. Optimization is carried out to determine the combining coefficients which results in low PAPR.A number of iterations are required to find the optimum phase rotation factor for different subblocks. Adaptive partial transmit sequence is proposed in[23] to reduce the number of iterations required to find optimum combination of factors for subblocks. Adaptive partial transmit sequence reduces the number of iteration by setting up a desired threshold and trial for different weighing factors until the PAPR drops under the threshold. Another

method in this category is the selective mapping scheme[19, 31]. In this N independent frames are generated representing the same information and the frame with lowest PAPR is used for transmission. The frames are generated by multiplying the same information with different phase vectors. Information about which particular data vector and transformation was used is sent as side information to the receiver. In the presence of noise there can be a problem with decoding the signal.

4.3.2.3 Tone Injection

The tone injection method for PAPR reduction is presented in [22]. The reduction signal also uses the data carrying tones, i.e. both the reduction as well as data carrying signal uses the same frequencies. But at the same time the constellation size is increased so that each point in the original basic constellation can be mapped into several equivalent points in the expanded constellation. On the receiver side the point is brought back to the original position by a modulo operation after the FFT. This method is called tone injection because substituting the points in the basic constellation for the new points in the extended constellation is equivalent to inject a new tone of suitable frequency and phase in the multicarrier symbol. This method has a few drawbacks e.g. side information for decoding the signal is required on the receiver side and due to an extra IFFT operation it is more complex. Also,it results in power increase in the transmit signal due to injected signal.

4.3.3 Wireless channel model and its power delay profile[32]

The physical mean to attribute a signal propagating in wireless channel is the power associated with it. The same signal reaches to destination at different time instants with different powers due to multipaths. The received signal is the sum of these reflected copies. Provided the system sampling rate, discrete time impulse response of the channel can be obtained from power delay profile of the channel. Therefore the channel can be modeled as an FIR filter $c(n)$ of length M, such that the associated power is $C(z)C^*(\frac{1}{z^*})$. In practical scenario the number of reflected signals may vary depending on whether one of the transmitter or the receiver or the causes of multipath is moving. For simplicity we assume that the channel, once sampled, has constant sample values.

The available delay samples in a channels power-delay profile are not necessarily the integer multiple of the input symbol duration. The transmission of input symbols over the channel with dissimilar delay profile leads to some loss in actual information. If T_s and T_c correspond to symbol duration and the channel duration respectively, then $T_c = kT_s(k \in \mathbb{N})$ to ensure high fidelity. But the power delay profile of various channels are available at fractional multiples of T_s. As an example, for the symbol rate of 12 Mbps, T_c comes out to be 83.3 ns. Rounding off the fractional values, as used in [34, 35], gives one approach of approximation. If multiple samples map to the same integral value, then it considers the average of all such samples at that point. But the power at any fractional sample is not necessarily same as that at the nearest integral due to the time variant nature of the channel.

So, the approach does not provide a perfectly viable solution.

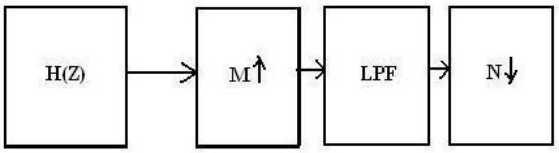

FIGURE 4.1: Power delay profile of channel reampled by $\frac{M}{N}$

Resampling the channel profile (demonstrated in Fig. 4.1) is an alternative to look at the issue. The following steps are adopted to attain the required sampling rate:

- Upsample the given profile by a factor M.
- Pass the interpolated profile through a Low pass filter with cutoff frequency $min(\frac{\pi}{M}, \frac{\pi}{N})$.
- Downsample the filtered response by a factor N.

4.4 Pulse shaping and Nyquist filter design

As the OFDM symbol consists of sum of signals of different amplitudes it leds to large PAPR and also the delay spread of the wireless communication channel caused by multipaths, introduces Inter Symbol Interference (ISI) in the transmitted signal. Presence of $M-1$ multipaths extends the input symbol $\mathbf{x}(n)$ of length N to the one with length $N+M-1$, which is the consequent overlap of individual pulses to the degree that the receiver can not reliably distinguish between individual signal elements. Instead of sending data at the sampling rate $F_s = \frac{1}{T_s}$, if it is transmitted at the rate $N.F_s$, the channel behaves as an impulse resulting no overlap of adjacent samples and also as the difference between individual pulses decreases peak fluctuations

decreases and hence PAPR decreases . Fig. 4.2 demonstrates the process described.

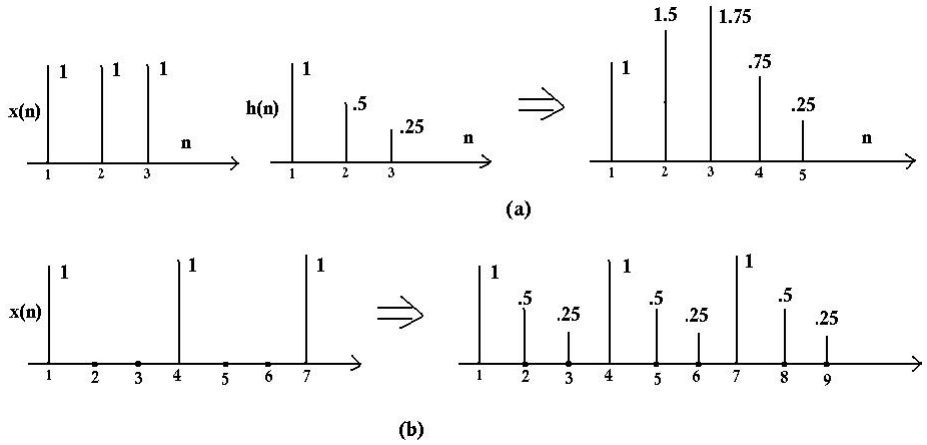

FIGURE 4.2: Demonstration of effect of channel for N=3 and M=3. **(a)**original signal convolved with channel **(a)**Upsampled signal convolved with channel

This can be achieved by interpolating $x(n)$ by a factor of M. But the process of upsampling adds images in the frequency spectrum of the signal, which can be suppressed by passing the upsampled signal through a low pass filter $w(n)$ with cut-off frequency $\frac{\pi}{M}$. The filtering operation can be made calculation efficient by decomposing the filter into M polyphase components as depicted in Fig. 4.3. The M-branch polyphase decomposition of $\mathbf{w}(z)$ is given by

$$\mathbf{w}(z) = \sum_{k=0}^{M-1} z^{-k}\mathbf{w}_k(z^M) \tag{4.7}$$

where

$$\mathbf{w}_k(z) = \sum_{n=-\infty}^{\infty} w(Mn+k)z^{-n}, \quad 0 \leq k \leq M-1 \tag{4.8}$$

Alternatively, the relation between $\mathbf{w}(n)$ and its each polyphase component in time domain is given by

$$w_k(n) = w(Mn+k), \quad 0 \leq k \leq M-1 \tag{4.9}$$

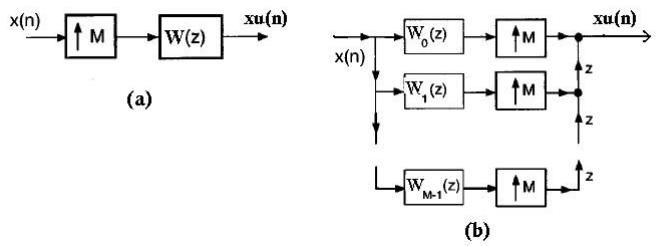

FIGURE 4.3: Interpolation filter $w(n)$ and its equivalent polyphase representation

The requirement is to get the original signal back with the sampling rate F_s, which can be attained by downsampling the received signal by M[30, 32]. To avoid the aliases caused by downsampling operation, the signal should be passed through a low-pass filter $w1(n)$ with cut-off frequency $\frac{\pi}{M}$ before downsampling. We are not completely done this way unless the cascade of filters, say $g(n) = w(n) * w1(n)$ satisfies Nyquist(M) criterion

$$\sum_{k=0}^{M-1} G(ze^{-j2\pi kf}) = M \tag{4.10}$$

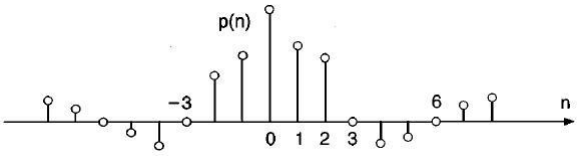

FIGURE 4.4: Nyquist(M) property of $G(Z)$ demonstrated for M=3

(4.10) expresses the Nyquist criterion in frequency domain. In time domain, it finds the form

$$g(n) = \begin{cases} 1 & n = 0 \\ 0 & n = nM,\ n \neq 0 \\ arbitrary & otherwise \end{cases} \tag{4.11}$$

i.e. there will be no ISI (ideally) between different symbols and the error in the transmission can be caused only by noise, if filter $g(n)$ has zero value at periodic intervals with period M and also PAPR reduces due to interpolation as shown in Fig. 4.4.

Fig. 4.5 describes the resulting communication channel.

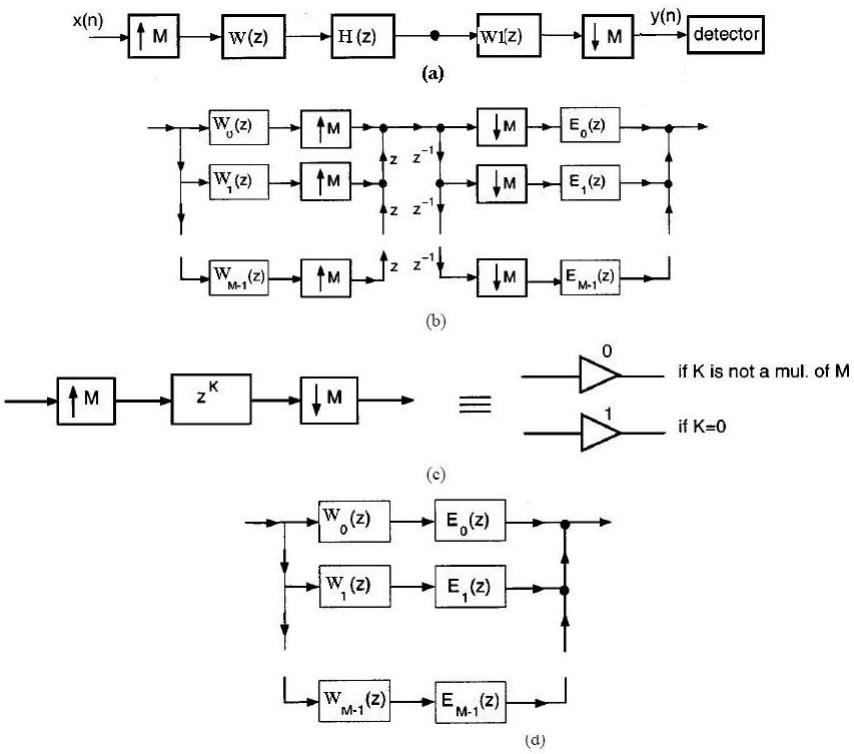

FIGURE 4.5: Considered digital equivalent of the communication channel. **(a)**Cascade of interpolator and decimator **(b)**Redrwaing in polyphse form **(c)**Basic multirate identity **(d)**Simplification of part (b) using the identity

4.4.1 Design of transmit and receive filter to meet Nyquist criterion

Nyquist pulse shaping is a crucial element in all bandwidth efficient digital communication systems using linear modulation techniques. Digital Nyquist pulse shaping is an application of multirate signal processing where the transmitter filter acts as an interpolator and the receiver filter can be considered

as a decimator. If $W1(Z) = W(Z^{-1})$, then the filter $W(Z)$ is known as square-root Nyquist(M) filter and the resulting filter $G(Z)$ can be given as

$$G(Z) = W(z)W(z^{-1}) \tag{4.12}$$

It is advantageous in the sense that if $W(Z)$ is linear phase, then the same filter can be employed at the transmitter as well as at the receiver embedded with some delay. The design of $W(Z)$ and $W1(Z)$ subject to the constraints of Nyquist filter, can be accomplished by different methods. One way is to design $G(Z)$ and then split it into two factors $W(Z)$ and $W1(Z)$ using any of the spectral factorization technique. Alternately, the constraints on $G(Z)$ can be expressed in terms of those on $W(Z)$ and then $W(Z)$ can be designed directly to meet those constraints. The latter strategy is adopted here for the design purpose.

4.4.1.1 Problem formulation

If the length of the root Nyquist filter is taken to be L, then it can be expressed as:

$$W(Z) = \sum_{n=0}^{L} w(n)z^{-n} \tag{4.13}$$

Let $\mathbf{w} = [w(0)\ w(1)\ \ldots\ w(L)]^T$ and $\mathbf{e}(z) = [1\ z^{-1}\ \ldots\ z^{-L}]^T$, then (4.13) can be written as

$$W(z) = \mathbf{w}^T\mathbf{e}(z) \tag{4.14}$$

Using (4.14) in (4.12), it transforms to

$$G(z) = \left(\mathbf{w}^T\mathbf{e}(z)\right)\left(\mathbf{w}^T\mathbf{e}(z^{-1})\right)^T$$

$$= \mathbf{w}^T\mathbf{e}(z)\mathbf{e}^T(z^{-1})\mathbf{w}$$

$$= \mathbf{w}^T\mathbf{R}(z)\mathbf{w} \tag{4.15}$$

where

$$\mathbf{R}(z) = \mathbf{e}(z)\mathbf{e}^T(z^{-1})$$

$$= \begin{pmatrix} 1 \\ z^{-1} \\ \vdots \\ z^{-L} \end{pmatrix}$$

$$= \sum_{n=-L}^{L} z^{-n}\mathbf{S}_n \tag{4.16}$$

$\mathbf{S}_n$ are constant matrices of size $(N+1)\ X\ (N+1)$, whose entries are given by

$$[\mathbf{S}_n]_{k,l} = \begin{cases} 1 & k-l=n \\ 0 & otherwise \end{cases} \tag{4.17}$$

Substituting (4.16) in (4.15), we obtain

$$G(z) = \sum_{n=-L}^{L} (\mathbf{w}^T\mathbf{S}_n\mathbf{w})z^{-n} \tag{4.18}$$

Now the set of constraints for $G(z)$ to be a Nyquist (M) filter can be defined in terms of $\mathbf{w}$ as

$$\mathbf{w}^T\mathbf{S}_n\mathbf{w} = \begin{cases} 1 & n=0 \\ 0 & n=nM,\ n\neq 0 \\ arbitrary & otherwise \end{cases} \tag{4.19}$$

$W(z)$ is a low pass filter, but some amount of energy will be distributed in the stop band of $W(Z)$ unless it is an infinite length filter, which is not attainable in practical cases. Therefore, the objective should be to minimize the energy over its stop band. Assuming a rolloff factor α for (square-root) raised-cosine filters , and recalling that $W(z)$ is to be designed for a sampling rate M times faster than the symbol rate, it can be found that the stopband of $W(z)$ starts at the normalized frequency

$$f_0 = \frac{1+\alpha}{2M} \tag{4.20}$$

and ends at $1 - f_0$. Following this, the cost function can be defined

$$\xi_s = \int_{f_0}^{1-f_0} |W(e^{j2\pi f})|^2 df \tag{4.21}$$

$$= \int_0^1 |W(e^{j2\pi f})|^2 df - \int_{-f_0}^{f_0} |W(e^{j2\pi f})|^2 df$$

$$= \mathbf{w}^T\mathbf{w} - \int_{-f_0}^{f_0} |W(e^{j2\pi f})|^2 df \tag{4.22}$$

since $\mathbf{w}^T\mathbf{w} = \int_0^1 |W(e^{j2\pi f})|^2 df$ according to Parseval's relation. As a part of design the aim is to minimize ξ_s.

Also

$$\int_{-f_0}^{f_0} |W(e^{j2\pi f})|^2 df = \int_{-f_0}^{f_0} \mathbf{w}^T\mathbf{e}(e^{j2\pi f})\mathbf{e}^T(e^{-j2\pi f})\mathbf{w} df$$

$$= \mathbf{w}^T\left(\int_{-f_0}^{f_0} \mathbf{e}(e^{j2\pi f})\mathbf{e}^T(e^{-j2\pi f}) df\right)\mathbf{w}$$

Therefore (4.22) can be rewritten as

$$\xi_s = \mathbf{w}^T\mathbf{\Phi}\mathbf{w} \tag{4.23}$$

where Φ is matrix of size $(N+1)\ X\ (N+1)$

$$\Phi = \mathbf{I} - \int_{-f_0}^{f_0} \mathbf{e}(e^{j2\pi f})\mathbf{e}^T(e^{-j2\pi f})df \tag{4.24}$$

Performing relevant integrals, the elements of Φ are obtained as

$$\phi_{kl} = \begin{cases} 1 - 2f_0 & k = l \\ -2f_0\ sinc(2f_0(k-l)) & k \neq l \end{cases} \tag{4.25}$$

Succinctly stating, the design of a root-Nyquist filter is performed by minimizing the cost function of (4.23), subject to the constraints (4.19).

4.4.1.2 Design procedure

The cost of realization of $W(z)$ can be reduced if it is designed to have a linear phase response. This is because linear phase translates to a symmetry in filter coefficients and this in turn cuts the number of multipliers down to one half. To include the symmetry of the filter coefficients in design formulation, the authors define the column vector $\mathbf{w}^{'}$ as

$$\mathbf{w}^{'} = [w(0)\ w(1)\ \ldots w((L-1)/2)]^T$$

when L is odd and

$$\mathbf{w}^{'} = [w(0)\ w(1)\ \ldots\ w((L)/2)]^T$$

when L is even. The vector $\mathbf{w}$ may be written in terms of $\mathbf{w}^{'}$ as

$$\mathbf{w} = \mathbf{E}\mathbf{w}^{'} \tag{4.26}$$

where $\mathbf{E} = \begin{bmatrix} \mathbf{I} \\ \\ \mathbf{J} \end{bmatrix}$, $\mathbf{I}$ is the identity matrix and $\mathbf{J}$, for L odd, is the antidiagonal matrix with entries 1 and, for L even, is obtained by removing the first row of the latter antidiagonal matrix. For L odd, the size of $\mathbf{E}$ is $(L+1)\ x\ (L+1)/2$.

Using (4.26), the constraints and cost function given by (4.19) and (4.23) respectively, can be rearranged as

$$\mathbf{w}^{'T}\mathbf{S}^{'}{}_{n}\mathbf{w}^{'} = \begin{cases} 1 & n = 0 \\ 0 & n = nM,\ n \neq 0 \\ arbitrary & otherwise \end{cases} \tag{4.27}$$

and

$$\xi_s = \mathbf{w}^{'T}\mathbf{\Phi}^{'}\mathbf{w}^{'} \tag{4.28}$$

where

$$\mathbf{S}^{'}{}_{n} = \mathbf{E}^T\mathbf{S}_n\mathbf{E} \tag{4.29}$$

and

$$\mathbf{\Phi}^{'} = \mathbf{E}^T\mathbf{\Phi}\mathbf{E} \tag{4.30}$$

The set of equations (4.27) can be written in compact form

$$\mathbf{B}\mathbf{w}^{'} \approx \mathbf{d} \tag{4.31}$$

where

$$\mathbf{B} = (\mathbf{I} \otimes \mathbf{h}^{'T})\mathbf{S}^{'} \tag{4.32}$$

$\otimes$ denotes Kronecher product, $\mathbf{I}$ is the identity matrix of size $L+1$,

$$\mathbf{S}^{'} = [\mathbf{S_0}^{'T}\ \mathbf{S_1}^{'T}\ \ldots\ \mathbf{S_L}^{'T}]^T \tag{4.33}$$

and

$$\mathbf{d} = [d_0\ d_1\ \ldots\ d_L]^T \tag{4.34}$$

Also, $\phi^{'}$ can be expanded as $\phi^{'} = \mathbf{C}^T\mathbf{C}$ by applying Cholesky factorization, where $\mathbf{C}$ is an upper triangular matrix. Thus, (4.28) can be rearranged as

$$\xi_s = (\mathbf{Cw}^{'})^T(\mathbf{Cw}^{'}) = ||(\mathbf{Cw}^{'})||^2 \tag{4.35}$$

Here, $||.||^2$ denotes the norm of a vector. From this, it can be said that as part of the design goal, we wish to find a vector $\mathbf{w}^{'}$ which satisfies the soft equation

$$\mathbf{Cw}^{'} \approx \mathbf{0} \tag{4.36}$$

where $\mathbf{0}$ is a column vector.

Combining (4.31) and (4.36), we get

$$\mathbf{Dw}^{'} \approx \mathbf{u} \tag{4.37}$$

where $\mathbf{D} = \begin{bmatrix} \mathbf{B} \\ \mathbf{C} \end{bmatrix}$ and $\mathbf{u} = \begin{bmatrix} \mathbf{d} \\ \mathbf{0} \end{bmatrix}$.

The approximation (4.37) is an over-determined system of soft equations for which we seek a solution for the unknown vector $\mathbf{w}^{'}$. Also, some of the rows of $\mathbf{D}$ contain linear combination of elements of $\mathbf{w}^{'}$, so (4.37) is quadratic in $\mathbf{w}^{'}$.

To solve (4.37), an error vector can be defined

$$\mathbf{v} = \mathbf{\Gamma}(\mathbf{D}\mathbf{w}^{'} - \mathbf{u}) \tag{4.38}$$

Here $\mathbf{\Gamma}$ is a diagonal matrix whose diagonal elements are set of weights given to elements of $\mathbf{D}\mathbf{w}^{'} - \mathbf{u}$. Larger weights are assigned to those elements whose minimization should be emphasized.

Optimum value of $\mathbf{h}^{'}$ is obtained by minimizing the norm of $\mathbf{v}$ i.e. the ultimate cost function is

$$\xi = ||\mathbf{v}||^2 \tag{4.39}$$

The filters designed adopting the so far discussed strategy turn to be fairly powerful in mitigating ISI as well as to maintain an acceptable level of Peak to Average Power Ratio (PAPR) at the transmitter output for ideal channel conditions.

Chapter 5

Discussion on Simulation Results

5.1 Simulation Results

The simulation results are divided into three parts.First, the proposed approach is compared to clipping technique used to reduce PAPR in OFDM.Secondly,the Peak to Average Power Ratio of an OFDM system is calculated for different modulation scheme by carrying out matlab simulation.Thirdly,RF amplifier characteristics for output power is plotted for different cases using RF toolbox in matlab.

The system considered for simulation is IEEE802.11aPHY(physical layer).Table 5.1 presents the parameters used for simulation. The channel considered are standardized channel for wireless LAN by Joint Technical Committee(JTC) and European Telecommunication Standards Institute(ETSI).Power delay profile for channel is given in AppendixA.

Parameter	**Value**
Input	Audio samples of 2Kb size
System Bandwidth	20MHz
Data Rate	54Mbps
Coding rate	3/4
SNR	2-20 dB with 3.14 dB increment and AWGN
Iterations	15 iterations per SNR value
CP duration	0.8 μs
Symbol duration	3.2 μs
Trans. symbol duration	4.0 μs
Bits per symbol	216
Frequency	5GHz

TABLE 5.1: Simulaion Parameters for IEEE802.11a PHY(Physical Layer)

5.1.1 PAPR Using Clipping

PAPR is calculated using an oversampling factor of 4. It was found that with a clipping level of 0.4 PAPR using clipping is 4.3644dB.However,by using pulse shaping technique(Square Root Nyquist(M)filter)we get a PAPR of 2.5605dB,hence a reduction of 1.8dB is achieved by using Square Root Nyquist(M)filter as an interpolating filter in an OFDM system.The PAPR using without filter is 6.5368dB which is 4dB more than pulse shaping technique and 2.2dB more than clipping technique.Fig5.1shows the comparison of BER vs SNR using clipping and pulse shaping technique to reduce PAPR.It was found that the performance of pulse shaping technique is much better than clipping technique.

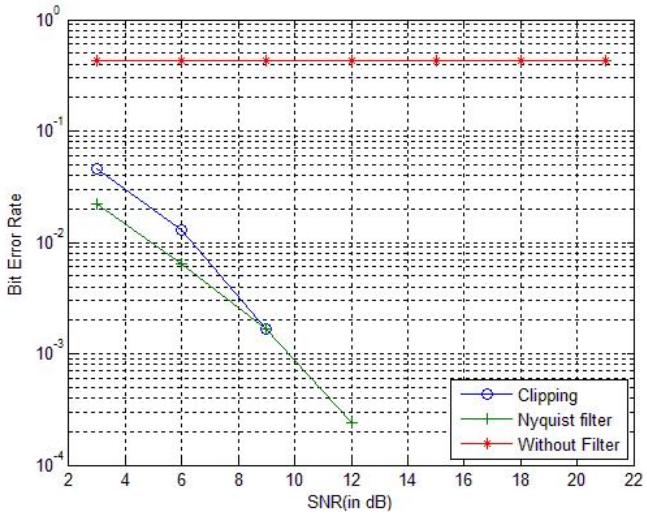

FIGURE 5.1: BER performance using clipping and Square Root Nyquist(M)filter

Oversampling Factor(M)	**PAPR without filter(in dB)**	**PAPR of Raised Cosine Filter(in dB)**	**PAPR Of Sqrt Nyquist(M) Filter(in dB)**
4	3.4858	2.4466	2.0332
6	3.4858	2.1802	2.0019
8	3.4858	2.0237	1.9374

TABLE 5.2: PAPR for BPSK modulation

5.1.2 PAPR for BPSK modulation

Peak to average power ratio for BPSK modulation is shown in Table 5.2 and it was found that PAPR decreases as oversampling factor increases.This is because increase in oversampling factor results in decrease in variation of peak amplitude as a result of which amount of fluctuation decreases and hence PAPR decreases. Bit error rate of an OFDM system is shown in Fig5.2 and it was found that a bit error value of 10^{-5} is attained at an SNR value of 12 dB in case of Nyquist M filter which is very less as compared to FIR root raised cosine filter and also without filter case. It is also found that bit error value for root raised cosine filter and without filter is not much affected by SNR value i.e. the input power has very less effect in this case.The PAPR of

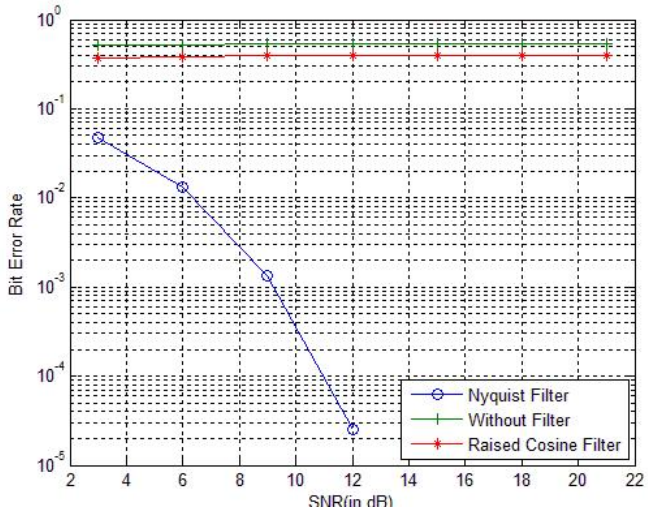

FIGURE 5.2: BER for BPSK modulation with oversampling factor M=4

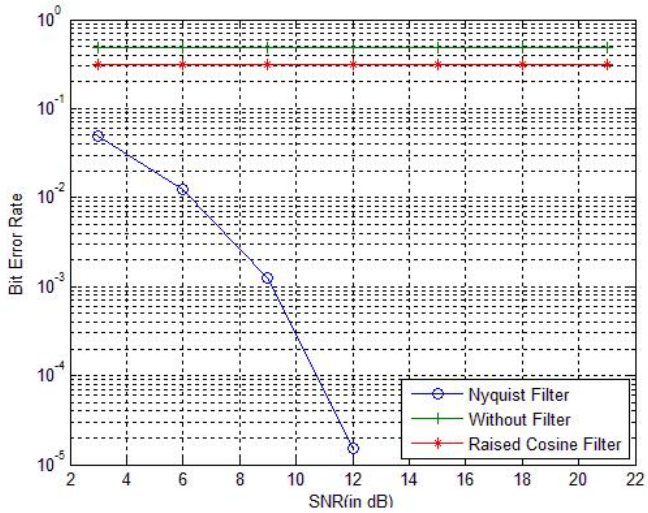

FIGURE 5.3: BER for BPSK modulation with oversampling factor M=6

square root Nyquist (M)filter is around .5db less than root raised cosine filter whereas if is around 1.5 db less than when OFDM symbols are transmitted at the symbol rate.The bit error rate for BPSK modulation with different oversampling factor is shown in Fig5.2-Fig5.4

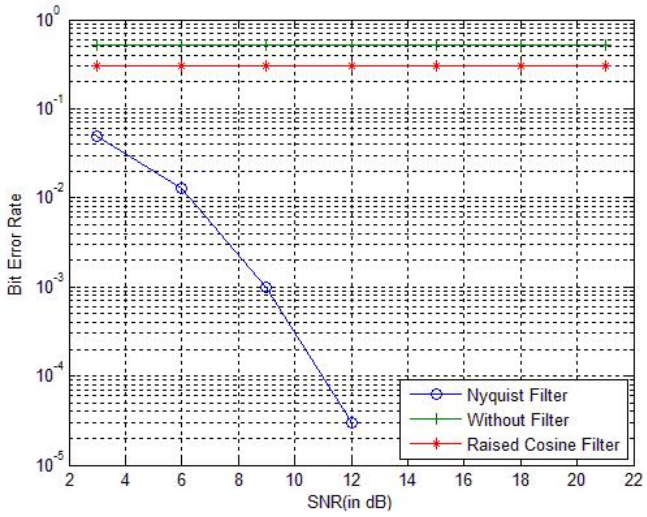

FIGURE 5.4: BER for BPSK modulation with oversampling factor M=8

Oversampling Factor(M)	**PAPR without filter(in dB)**	**PAPR of Raised Cosine Filter(in dB)**	**PAPR Of Sqrt Nyquist(M) Filter(in dB)**
4	3.9785	3.8969	3.3345
6	3.9785	3.8333	3.1506
8	3.9785	3.7660	3.0285

TABLE 5.3: PAPR for 16-QAM modulation

5.1.3 PAPR for 16-QAM modulation

Peak to average power ratio for 16-QAM modulation is shown in Table 5.3 and it was found that PAPR decreases as oversampling factor increases.This is because increase in oversampling factor results in decrease in variation of peak amplitude as a result of which amount of fluctuation decreases and hence PAPR decreases. Bit error rate of an OFDM system is shown in Fig5.5 and it was found that a bit error value of Nyquist M filter is very less as compared to compared to FIR root raised cosine filter and also without filter case.The PAPR of square root Nyquist (M)filter is around .5db less than root raised cosine filter whereas if is around .6 db less than when OFDM symbols are transmitted at the symbol rate.The bit error rate for 16QAM modulation

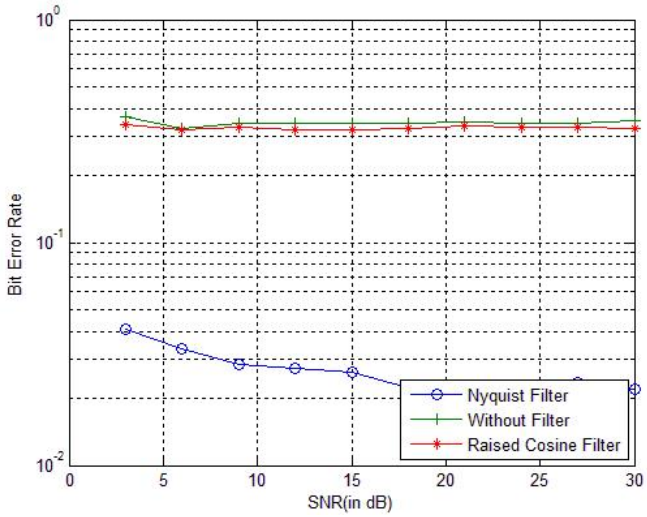

FIGURE 5.5: BER for 16-QAM modulation with oversampling factor M=4

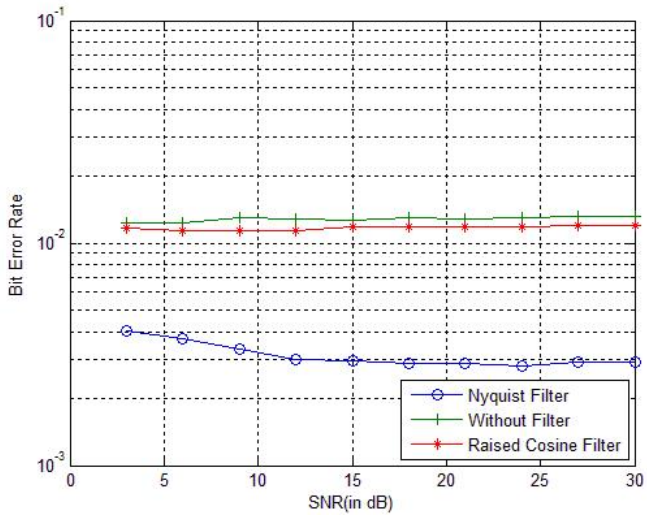

FIGURE 5.6: BER for 16-QAM modulation with oversampling factor M=6

with different oversampling factor is shown in Fig5.5-Fig5.7

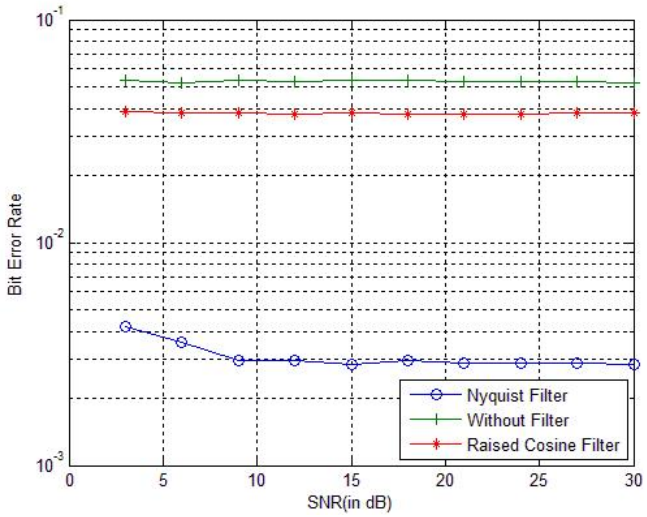

FIGURE 5.7: BER for 16-QAM modulation with oversampling factor M=8

Oversampling Factor(M)	**PAPR without filter(in dB)**	**PAPR of Raised Cosine Filter(in dB)**	**PAPR Of Sqrt Nyquist(M) Filter(in dB)**
4	4.0785	3.8969	3.3345
6	4.0785	3.8333	3.1506
8	4.0785	3.7660	3.0285

TABLE 5.4: PAPR for 64-QAM modulation

5.1.4 PAPR for 64-QAM modulation

Peak to average power ratio for 64-QAM modulation is shown in Table 5.2 and it was found that PAPR decreases as oversampling factor increases.This is because increase in oversampling factor results in decrease in variation of peak amplitude as a result of which amount of fluctuation decreases and hence PAPR decreases. Bit error rate of an OFDM system is shown in Fig5.8 and it was found that a bit error value of Nyquist M filter is very less as compared to FIR root raised cosine filter and also without filter case.The PAPR of square root Nyquist (M)filter is around .5db less than root raised cosine filter whereas if is around .7 db less than when OFDM symbols are

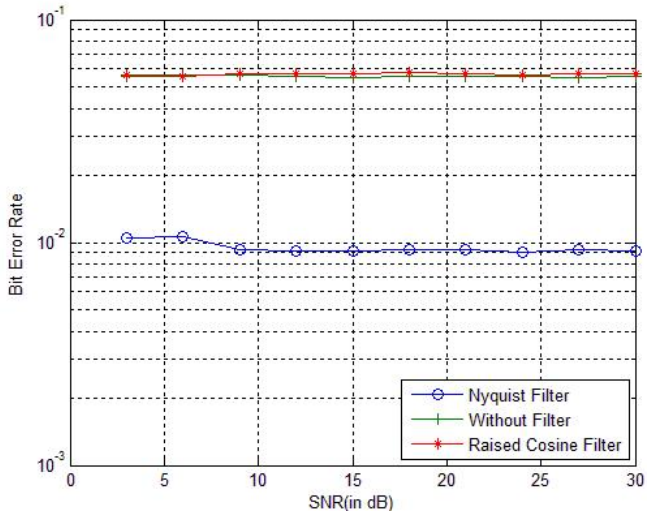

FIGURE 5.8: BER for 64-QAM modulation with oversampling factor M=4

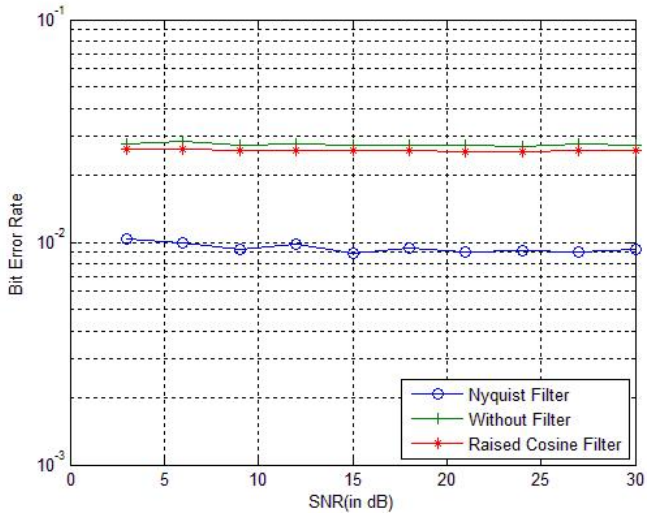

FIGURE 5.9: BER for 64-QAM modulation with oversampling factor M=6

transmitted at the symbol rate.The bit error rate for 64-QAM modulation with different oversampling factor is shown in Fig5.8-Fig5.10

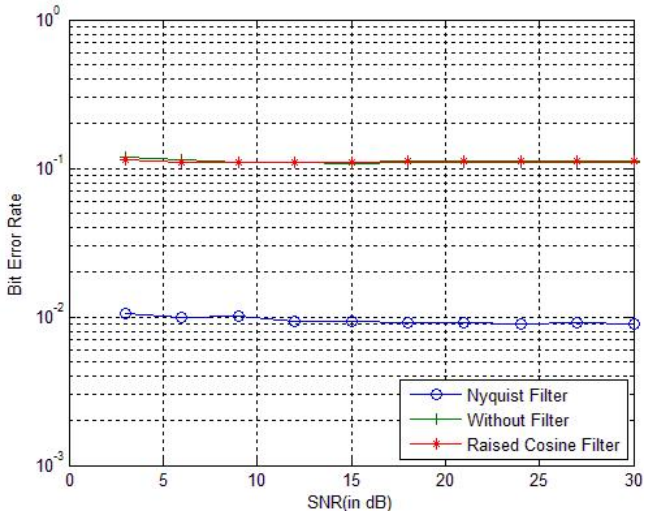

FIGURE 5.10: BER for 64-QAM modulation with oversampling factor M=8

Oversampling Factor(M)	**PAPR without filter(in dB)**	**PAPR of Raised Cosine Filter(in dB)**	**PAPR Of Sqrt Nyquist(M) Filter(in dB)**
4	5.1926	4.1870	3.8702
6	5.1926	4.1202	3.6301
8	5.1926	4.0515	3.5121

TABLE 5.5: PAPR for 256-QAM modulation

5.1.5 PAPR for 256-QAM modulation

Peak to average power ratio for 256-QAM modulation is shown in Table 5.2 and it was found that PAPR decreases as oversampling factor increases.This is because increase in oversampling factor results in decrease in variation of peak amplitude as a result of which amount of fluctuation decreases and hence PAPR decreases. Bit error rate of an OFDM system is shown in Fig5.2 and it was found that a bit error value of Nyquist M filter is very less as compared to FIR root raised cosine filter and also without filter case.The PAPR of square root Nyquist (M)filter is around .3db less than root raised cosine filter whereas if is around 1.2 db less than when OFDM symbols are transmitted at the symbol rate.The bit error rate for 256-QAM modulation

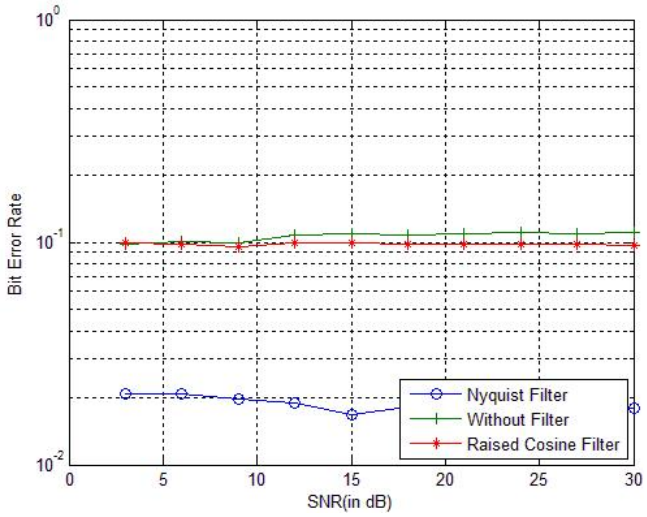

FIGURE 5.11: BER for 256-QAM modulation with oversampling factor M=4

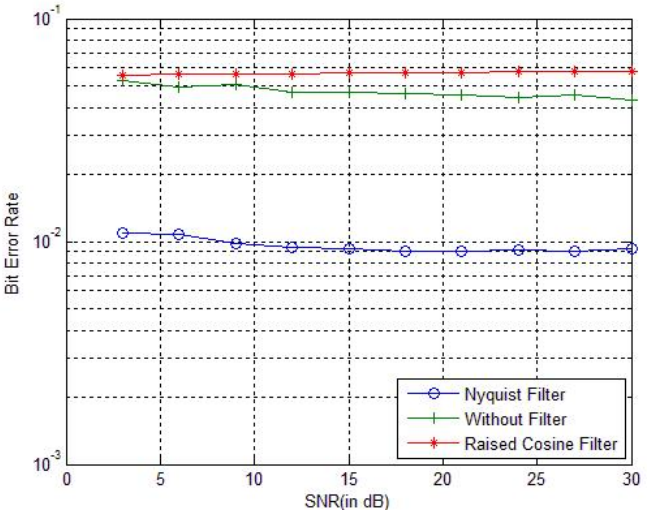

FIGURE 5.12: BER for 256-QAM modulation with oversampling factor M=6

with different oversampling factor is shown in Fig5.11-Fig5.13

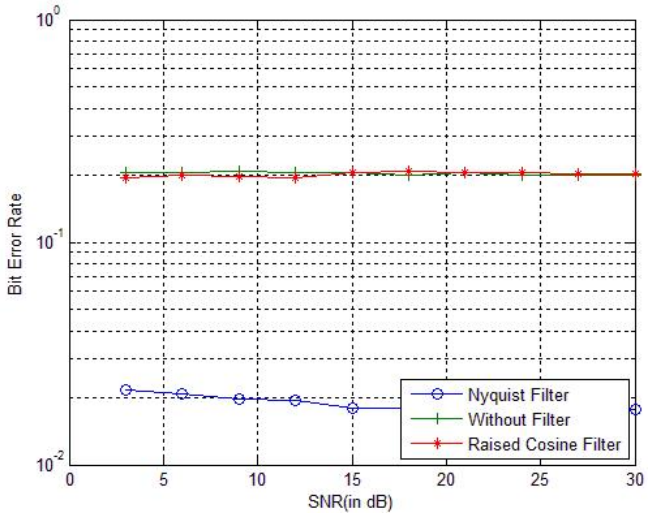

FIGURE 5.13: BER for 256-QAM modulation with oversampling factor M=8

5.1.6 RF Amplifier Characteristics

The RF amplifier characteristics for the various cases is shown in Fig5.15-Fig5.17.The reference amplifier has a dynamic range of 20dbm and a gain of 20dB at 5GHz frequency as shown in Fig5.14.It was found that 150dBm of input power gets clipped in case of an OFDM system without filter as shown in Fig5.17.In case of Root Raised Cosine filter 20dBm of input power gets clipped as shown in Fig5.16.The amount of clipping in case of Square Root Nyquist M filter is very less as compared to others.It is around 10dBm in case of Nyquist M filter as shown in Fig5.15.Thus in band distortion(constellation tilting and scattering),out-of-band distortion(spectral regrowth) and back off(ratio of saturation power to average input power) are much less in case of Nyquist M filter as compared to others.

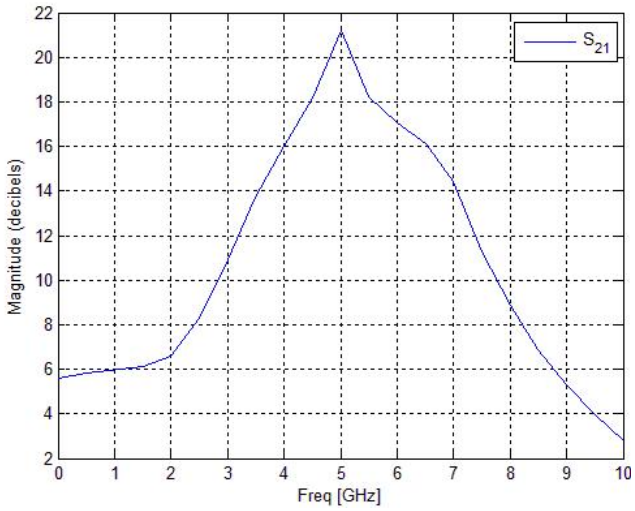

FIGURE 5.14: Gain characteristics of amplifier

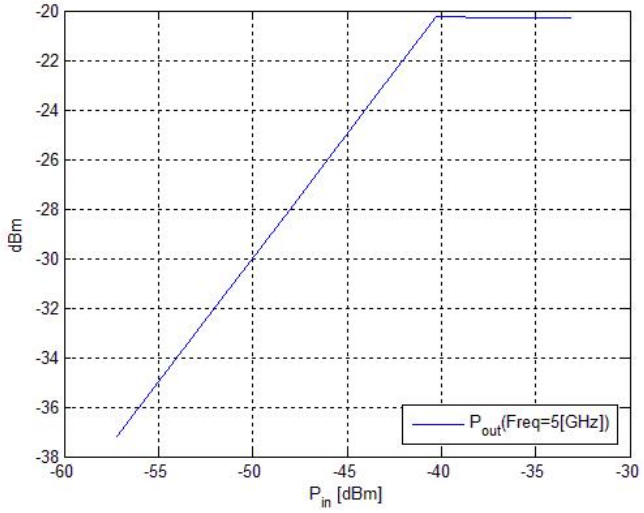

FIGURE 5.15: PIN vs POUT characteristics of amplifier with Nyquist(M) filter

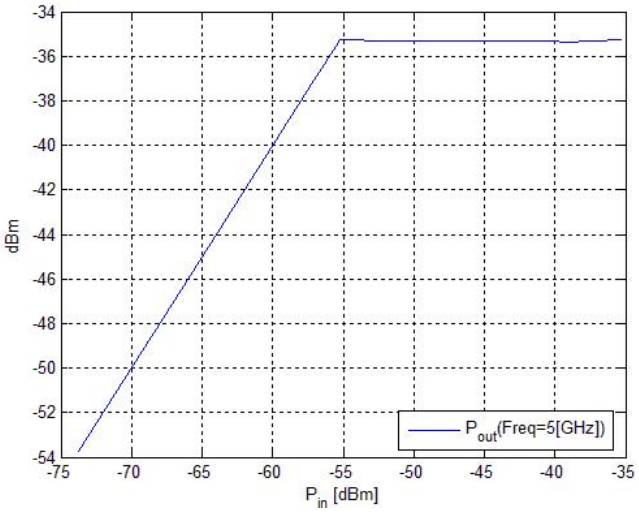

FIGURE 5.16: PIN vs POUT characteristics of amplifier with Raised Cosine filter

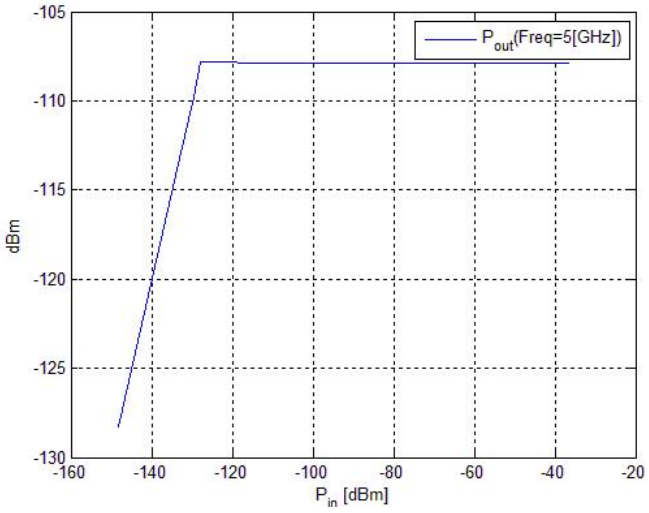

FIGURE 5.17: PIN vs POUT characteristics of amplifier with out filter

Chapter 6

Conclusion and Direction

6.1 Conclusion

PAPR for various modulation schemes and using different type of filters are calculated and it was found that PAPR of Square Root Nyquist M filter is lower than Root Raised Cosine Filter which in turn is lower than without filter . It is also found that PAPR decreases as the oversampling factor is increased.BER vs SNR for each case is also shown in the simulation results.It was also found that BER value for QAM modulation is less affected by SNR value as compared to BPSK modulation.PAPR value increases as the order of modulation increases because amplitude fluctuation increases as a result of which PAPR increases.The amount of nonlinear distortion decreases in case of Nyquist M filter.

6.2 Future Direction

- Reduction of PAPR concept can be extended to the case of MIMO channels.

- The algorithm we have used for PAPR reduction is based on minimum mean square minimization problem.It can be extended to minimax condition.
- The filter used for reduction of PAPR is an FIR filter.It can be designed for IIR case.

Appendix A

Power Delay Profile of Channels

The tables given below refer to the power delay profile of the channels that we have considered for simulation. All the delay values are in *nano seconds* and powers are in dB.

Delay	**Power**	**Delay**	**Power**	**Delay**	**Power**
0	-2.6	110	-2.6	380	-12.1
10	-3.0	140	-3.9	430	-14.3
20	-3.5	180	-3.4	490	-15.4
30	-3.9	230	-5.6	560	-18.4
50	0.0	280	-7.7	640	-20.7
80	-1.3	330	-9.9	730	-24.6

Table A.1: Power-Delay Profile of ETSI[2] channel

Delay	**Power**	**Delay**	**Power**
0	0	325	-10.1
50	-1.6	550	-17.1
150	-4.7	700	-21.7

Table A.2: Power-Delay Profile of JTC[B] channel

Bibliography

[1] P.P. Vaidyanathan, "A tutorial on multirate digital filter banks", (invited paper) ISCAS, 1988.

[2] M. Vetterli, "A Theory of Multirate Filter Banks", in *IEEE Trans. Acoust., Speech, and Signal Proc.*, vol. 35, pp. 356-372, Mar. 1987.

[3] Sanjit K. Mitra, *Digital signal processing*, Third edition, Tata McGraw-Hill publications.

[4] P. P. Vaidyanathan *Multirate systems and filter banks*, Prentice Hall Signal processing Series, 2004.

[5] P.P. Vaidyanathan, "Quadrature mirror filter banks, M-band Extensions, and Perfect Reconstruction techniques", in *IEEE ASSP Mag.*, vol. 4, pp. 4-20, Jul. 1987.

[6] P.P. Vaidyanathan, "Multirate digital filters, filter banks, polyphase networks, and applications: A tutorial", in *Proc. IEEE*, vol. 78, pp. 56-93, Jan. 1990.

[7] M. Vetterli, "Perfect Transmultiplexers", ICASSP, 1986.

[8] Gregory W. Wornell, "Emerging applications of multirate signal processing and wavelets in digital communications", in *Proceedings of the IEEE*, vol. 84, no. 4, Apr. 1996.

[9] D. S.Waldhauser and J. A. Nossek, "Multicarrier systems and filter banks", Adv. Radio Sci., 4, 165169, 2006.

[10] See-May Phoong, Yug Chang, and Chun-Yang Chen, "DFT-Modulated Filterbank Transceivers for Multipath Fading Channels", in *IEEE Trans. Signal Processing.*, vol. 53, no. 1, Jan. 2005.

[11] Teijun Wang, John G. Proakis and James R. Zeidler "Techniques for suppression of inter-carrier interference in OFDM systems", in *IEEE Communications Society*, Feb. 2005.

[12] John A. C. Bingham, "Multicarrier Modulation for Data Transmission: An Idea Whose Time Has Come", in *IEEE Communications Magazine*, May 1990.

[13] Borton R. Saltzberg, "Comparison of single-carrier and multitone digital modulation for ADSL applications", in *IEEE Communications magazine*, Nov. 1998.

[14] A. J. Redfern, "Receiver window design for multicarrier communication systems", in *IEEE J. Sel. Areas Commun.*, pp. 10291036, June 2002.

[15] R. W. Lowdermilk, "Design and performance of fading insensitive orthogonal frequency division multiplexing (OFDM) using polyphase filtering techniques", in *Conf. Rec. Thirtieth Asilomar Conf. Signals, Systems Computers*, Nov. 1996.

[16] A. Vahlin and N. Holte, "Optimal finite duration pulses for OFDM", IEEE Trans. Commun., vol. 44, pp. 1014, Jan. 1996.

[17] P. Siohan, C. Siclet, and N. Lacaille, "Analysis and design of OFDM/OQAM systems based on filter bank theory", in *IEEE Transactions on Signal Processing*, vol. 50, no. 5, pp. 11701183, 2002.

[18] Behrouz Farhang-Boroujeny, "A Square-Root Nyquist (M) Filter Design for Digital Communication Systems", presented in *Software Defined Radio Technical Conf., Orlando*, Nov. 2006.

[19] Mller, S. H. Huber, "J. B. A Comparison Of Peak Power Reduction Schemes For OFDM ", in Proc *IEEE GlobeCom*, 1997, 1-5.

[20] Blcskei, H.; Duhamel, P. Hleiss, R. "Orthogonalization of OFDM/OQAM pulse shaping filters using the discrete Zak transform Signal Process",*Elsevier North-Holland, Inc.*, 2003, 83, 1379-1391.

[21] Haider, K. "Peak to Average Ratio Reduction in Wireless OFDM communication Systems", Blekinge institute of Technology, 2006

[22] Han, S. H. Lee, J. H., "An overview of peak-to-average power ratio reduction techniques for multicarrier transmission Wireless Communications",*Wireless Communications, IEEE* , 2005, 12, 56-65.

[23] Jayalath, A. Tellambura, C.,"Adaptive PTS approach for reduction of peak-to-average power ratio of OFDM signal",*Electronics Letters*, 2000, 36, 1226-1228.

[24] Cavalcante ,R. Yamada, I.," A flexible peak-to-average power ratio reduction scheme for OFDM systems by the adaptive projected subgradient method",*IEEE Transactions on Signal Processing*, 2009.

[25] Jiao, Y.; Liu, X. Wang, X.,"A Novel Tone Reservation Scheme with Fast Convergence for PAPR Reduction in OFDM Systems",*Consumer Communications and Networking Conference*, 2008. CCNC 2008. 5th IEEE, 2008, 398-402.

[26] A.E. Jones, T.A Wilkinson, and S.K. Barton, "Block coding scheme for reduction of peak to mean envelope power ratio of multicarrier transmission schemes", *Electronics Letters*, Vol.30, No. 25, pp. 2098-2099, Dec.1994.

[27] S.H. Muller, and J.B. Huber, "OFDM with Reduced Peak to Average Power Ratio by Optimum Combination of Partial Transmit Sequences". *IEEE Electronics Letters*, Vol. 33, No. 5, pp 368-369 February, 1997.

[28] Liu, W.-R.,"Clipping Noise Cancellation for OFDM Systems with Clipped Data Signals",*College of Electrical Engineering and Computer Science National Central University*, 2008.

[29] Pfletschinger, S.,"Multicarrier Modulation for Broadband Return Channels in Cable TV Networks",*Institut fr Nachrichtenbertragung der Universitt Stuttgart*, 2003.

[30] F. Mintzer, "On half-band, third-band and Nth band FIR filters and their design",*IEEE Trans.ASSP*,pp.734-738, Oct. 1982.

[31] C. L. Wang, Y. Ouyang and H. C. Chen, "A low-complexity peak-to-average power ratio reduction technique for OFDM-based systems",*in*

Proc. 60th IEEE Vehicular Technology Conference, September 26-29,2004, vol. 6, pp. 4380-4384.

[32] Arya, K.,"MULTIRATE SIGNAL PROCESSING IN DIGITAL COMMUNICATIONS", DA-IICT, 2008.

[33] Xiong, F.," Digital Modulation Techniques", *Second Edition (Artech House Telecommunications Library) Artech House, Inc.*, 2006.

[34] Sun-Wook Kim, Kyun Hyon Tchah, "Performance analysis of adaptive equalizer design for OFDM wireless LAN", in *IEEE Transactions on Consumer Electronics*, vol. 50, no. 2, May 2004.

[35] Pravin Patidar and Dr. C. Vijaykumar "A model based channel shortening technique for IEEE 802.11a OFDM system", in *IEEE TENCON 2007*, Taipei international convention center, Taipei, Taiwan.